



Another look at the foramen magnum in bipedal mammals[☆]



Gabrielle A. Russo^{a, *}, E. Christopher Kirk^{b, c}

^a Department of Anthropology, Stony Brook University, Stony Brook, NY 11794, USA

^b Department of Anthropology, The University of Texas at Austin, Austin, TX 78712, USA

^c Jackson School Museum of Earth History, The University of Texas at Austin, Austin, TX 78712, USA

ARTICLE INFO

Article history:

Received 16 July 2016

Accepted 26 January 2017

Keywords:

Basicranium

Bipedalism

Comparative method

Human evolution

ABSTRACT

A more anteriorly positioned foramen magnum evolved in concert with bipedalism at least four times within Mammalia: once in macropodid marsupials, once in heteromyid rodents, once in dipodid rodents, and once in hominoid primates. Here, we expand upon previous research on the factors influencing mammalian foramen magnum position (FMP) and angle with four new analyses. First, we quantify FMP using a metric (basioccipital ratio) not previously examined in a broad comparative sample of mammals. Second, we evaluate the potential influence of relative brain size on both FMP and foramen magnum angle (FMA). Third, we assess FMP in an additional rodent clade (Anomaluroidea) containing bipedal springhares (*Pedetes* spp.) and gliding/quadrupedal anomalures (*Anomalurus* spp.). Fourth, we determine the relationship between measures of FMP and FMA in extant hominoids and an expanded mammalian sample. Our results indicate that bipedal/orthograde mammals have shorter basioccipitals than their quadrupedal/non-orthograde relatives. Brain size alone has no discernible effect on FMP or FMA. Brain size relative to palate size has a weak influence on FMP in some clades, but effects are not evident in all metrics of FMP and are inconsistent among clades. Among anomaluroids, bipedal *Pedetes* exhibits a more anterior FMP than gliding/quadrupedal *Anomalurus*. The relationship between FMA and FMP in hominoids depends on the metric chosen for quantifying FMP, and if modern humans are included in the sample. However, the relationship between FMA and FMP is nonexistent or weak across rodents, marsupials, and, to a lesser extent, strepsirrhine primates. These results provide further evidence that bipedal mammals tend to have more anteriorly positioned foramina magna than their quadrupedal close relatives. Our findings also suggest that the evolution of FMP and FMA in hominins may not be closely coupled.

© 2017 Elsevier Ltd. All rights reserved.

1. Introduction

An anteriorly positioned foramen magnum has long been recognized as a distinctive feature of humans compared to other primates (Daubenton, 1764; Broca, 1872; Topinard, 1890). Questions regarding foramen magnum position (herein, FMP) and orientation remain the subject of vigorous debate in biological anthropology, particularly with regard to proposed links to other structural and/or functional systems in the body (e.g., locomotion, trunk and/or head posture, brain expansion and/or reorganization; e.g., Biegert, 1957, 1963; Kimbel and Rak, 2010; Russo and Kirk, 2013; Ruth et al.,

2016). As a result, little consensus has emerged regarding the possibility that the anteriorly positioned foramina magna of some fossil species are functionally associated with bipedal locomotion and/or orthograde trunk postures (e.g., Dart, 1925; White et al., 1994; Brunet, 2002; Brunet et al., 2002; Wolpoff et al., 2002, 2006; Kimbel et al., 2004; Guy et al., 2005; Suwa et al., 2009; Kimbel and Rak, 2010; Russo and Kirk, 2013; Kimbel et al., 2014; Ruth et al., 2016). In a previous study, we demonstrated that a more anteriorly-positioned foramen magnum evolved in concert with bipedalism at least four times within Mammalia: once in macropodid marsupials, once in heteromyid rodents, once in dipodid rodents, and once in hominoid primates (Russo and Kirk, 2013). To do so, we quantified the position of basion (the anteriormost margin of the foramen magnum at midline) relative to three osteological landmarks (the distalmost molar, the posteriormost aspect of the bony palate at midline, and the anteriormost aspect of the temporal fossa) that could be reliably identified on a

[☆] Funding sources: The Leakey Foundation.

* Corresponding author.

E-mail addresses: gabrielle.russo@stonybrook.edu (G.A. Russo), eckirk@austin.utexas.edu (E.C. Kirk).

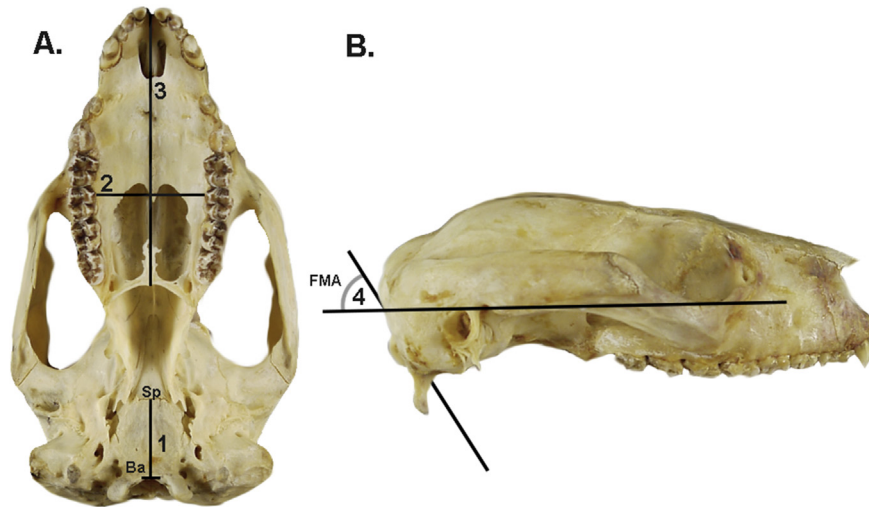


Figure 1. Measurements taken on each mammal cranium photographed in norma basilaris (A) and norma lateralis (B). Measurement 1: distance between basion (Ba) and the speno-occipital synchondrosis at the midline (i.e., spenobasion;Sp). Measurement 2: palate width measured as the maximum transverse distance across the bony palate to the lingualmost surface of the cheek teeth. Measurement 3: palate length measured as the linear distance between prosthion and staphylion. Measurement 4: foramen magnum angle (FMA) measured as the angle between a straight edge aligned with the opisthion – basion chord and the Frankfort Horizontal. Crania shown belong to *Pseudochirops archeri*.

taxonomically and morphologically diverse comparative sample (Russo and Kirk, 2013). Having established an association between anteriorly positioned foramina magna and bipedal locomotion across several distantly related mammalian lineages, we interpreted our results as providing support for the utility of foramen magnum position as an indicator of bipedal locomotion in fossil hominins (Russo and Kirk, 2013).

Ruth et al. (2016) recently challenged our findings, arguing that our metrics (molar ratio, palate ratio, and temporal fossa ratio) do not accurately capture FMP but instead correspond to size changes in other regions of the skull. Specifically, they asserted that masticatory apparatus size in marsupials, auditory bulla size in rodents, and brain size in strepsirrhine primates are confounding factors that account for the differences we observed between bipedal and quadrupedal mammals. After rejecting the utility of our metrics for quantifying FMP position in mammals, Ruth et al. (2016) derived a measure of foramen magnum orientation (called “foramen magnum angle”, or “FMA”) that they claim represents both the foramen magnum’s anteroposterior location and inclination. Ruth et al. (2016) observed that FMA did not differ between bipedal and quadrupedal marsupials. Although FMA did distinguish between bipedal and quadrupedal rodents, they found that this relationship was no longer significant when auditory bulla size was included as a predictor variable. Based on these findings, Ruth et al. (2016) concluded that locomotion does not influence either FMA or FMP. Here, we expand upon previous research on the factors influencing mammalian FMP and FMA with four new analyses.

1.1. Study objectives

1.1.1. Objective #1 Given the claim that our original metrics for quantifying FMP were biased by the choice of landmarks associated with mastication (Ruth et al., 2016), we first sought to quantify FMP using an alternate reference landmark that is not expected to directly capture changes in the size or position of masticatory structures. To this end, we selected the speno-occipital synchondrosis for assessing FMP because it is (1) readily visible across a wide range of mammalian taxa (see below and Fig. 1), (2) located along the midline axis of the basicranium, and (3) not inherently a masticatory structure. Accordingly, we measured

basion relative to the speno-occipital synchondrosis¹ for the entire comparative sample from our former study (Russo and Kirk, 2013) (Tables 1 and 2; see also Fig. S1 in the Supplementary Online Material [SOM]). These data provide an opportunity to test if bipedal and orthograde mammals differ from their quadrupedal and non-orthograde close relatives in exhibiting a forward translation of the foramen magnum associated with a decrease in basioccipital length.

1.1.2. Objective #2 Our second objective was to further examine the influences of brain size and masticatory apparatus size on FMP and FMA. In our previous analysis (Russo and Kirk, 2013), we found that orthograde strepsirrhines have more anteriorly positioned foramina magna than non-orthograde strepsirrhines. Ruth et al. (2016) called this result into question, claiming instead that our findings for strepsirrhines were the result of interspecific differences in relative brain size rather than in trunk posture. To reach this conclusion, Ruth et al. (2016) examined the relationship between FMA and the ratio of brain weight to body weight (their “encephalization ratio” or ER). As relative brain size has long been considered a factor that is likely to influence basicranial anatomy (e.g., Biegert, 1957, 1963), we examined the relationship between FMP, FMA, and encephalization quotient (EQ). We chose to measure relative brain size using EQ rather than ER because the relationship between brain size and body size is negatively allometric among mammals (Jerison, 1973; Martin, 1981), leading to systematic variation in ER according to body size. In contrast to ER, EQ facilitates comparisons across a range of body sizes by describing the difference between a species’ observed brain size and the brain size expected for its body size (Boddy et al., 2012). We also calculated multiple metrics of brain size relative to palate length and width (Table 2) to improve resolution of how FMA and FMP relate to relative brain size as envisioned by Biegert (1957, 1963), whose hypothesis specifically concerns brain size relative to masticatory apparatus size. In doing so, we seek to improve the study by Ruth et al. (2016) by increasing the size of the comparative sample, by

¹ Equivalent to basioccipital length, or the distance from basion to spenobasion.

Table 1
Mammal cranial metrics (species means).

Order Family	Species	Common name	L or P	Cranial size	Palate ratio	Molar ratio	Temporal fossa ratio	Basioccipital ratio	FMA ^a	ECV	B/ PL	B/ PLW	EQ ^b	BI	WI
Diprotodontia															
Macropodidae															
	<i>Dendrolagus lumholtzi</i>	Lumholtz's Tree Kangaroo	Q	74.0	0.48	0.48	0.62	0.22	49.69	26.2	0.54	0.87	0.68* ¹	–	–
	<i>Dendrolagus matschei</i>	Matschie's Tree Kangaroo	Q	76.8	0.51	0.51	0.67	0.25	44.55*	27.5	0.51	0.87	0.62* ¹	–	–
	<i>Dorcopsis hageni</i>	New Guinean Forest Wallaby	B	76.7	0.54	0.55	0.59	0.21	44.24	22.5	0.42	0.77	0.68* ¹	–	–
	<i>Macropus eugenii</i>	Tammar Wallaby	B	62.3	0.47	0.47	0.59	0.18	45.97	23.7	0.57	1.04	0.84	–	–
	<i>Macropus giganteus</i>	Eastern Gray Kangaroo	B	127.3	0.43	0.48	0.52	0.15	48.99	69.8	0.34	0.67	0.45	–	–
	<i>Macropus irma</i>	Western Brush Wallaby	B	80.2	0.43	0.43	0.50	0.17	49.93*	24.7	0.42	0.75	0.77* ¹	–	–
	<i>Macropus robustus</i>	Wallaroo	B	119.2	0.41	0.47	0.52	0.17	53.52	59	0.36	0.67	0.44	–	–
	<i>Macropus rufogriseus</i>	Red-necked Wallaby	B	77.7	0.44	0.45	0.54	0.16	70.73	36	0.50	0.90	0.61	–	–
	<i>Macropus rufus</i>	Red Kangaroo	B	129.8	0.41	0.47	0.53	0.16	46	62.4	0.33	0.61	0.37	–	–
	<i>Onychogalea lunata</i>	Crescent nail-tailed wallaby	B	55.1	0.44	0.39	0.49	0.16	39.84*	10.2	0.65	1.01	0.82* ¹	–	–
	<i>Setonix brachyurus</i>	Quokka	B	68.0	0.47	0.47	0.61	0.19	–	13.9	0.47	0.80	0.62* ¹	–	–
	<i>Thylogale stigmatica</i>	Red-legged Pademelon	B	60.7	0.45	0.43	0.56	0.16	50.71	17.8	0.53	0.95	0.60* ¹	–	–
	<i>Wallabia bicolor</i>	Swamp Wallaby	B	80.7	0.44	0.41	0.56	0.18	73.69	32.9	0.49	0.87	0.42	–	–
Petauridae	<i>Petaurus breviceps</i>	Sugar Glider	Q	30.2	0.41	0.53	0.66	0.18	–	2.09	0.65	1.08	1.23* ¹	–	–
Phalangeridae															
	<i>Ailurops ursinus</i>	Large Celebes Cuscus	Q	63.9	0.51	0.50	0.70	0.19	55.73 ^a	16.17 ^a	0.58	0.88	0.61* ¹	–	–
	<i>Phalanger orientalis</i>	Northern Common Cuscus	Q	51.0	0.50	0.50	0.69	0.17	41.72	6.43	0.50	0.90	0.61	–	–
	<i>Spilogiscus maculatus</i>	Spotted Cuscus	Q	74.8	0.44	0.46	0.66	0.19	63.90	13.4	0.43	0.75	0.61	–	–
	<i>Trichosurus vulpecula</i>	Brush-tailed Possum	Q	61.4	0.60	0.53	0.63	0.18	48.06	11	0.54	0.94	0.77	–	–
Phascolarctidae	<i>Phascolarctos cinereus</i>	Koala	Q	87.1	0.61	0.65	0.79	0.17	54.13	20.02	0.47	0.82	0.57* ¹	–	–
Potoroidae															
	<i>Aepyprymnus rufescens</i>	Rufous 'Rat'-kangaroo	B	61.7	0.40	0.41	0.60	0.16	47.92*	12.3	0.47	0.76	0.58* ¹	–	–
	<i>Bettongia penicillata</i>	Short-nosed 'Rat'-kangaroo	B	52.7	0.40	0.42	0.61	0.16	46	9.56	0.48	0.84	1.04	–	–
	<i>Potorous tridactylus</i>	Potoroo	Q	49.3	0.45	0.48	0.61	0.14	38.82	9.53	0.50	0.95	0.79* ¹	–	–
Pseudocheiridae															
	<i>Petauroides volans</i>	Greater Gliding Possum	Q	40.1	0.50	0.49	0.64	0.15	49.61	4.69	0.59	1.02	0.54	–	–
	<i>Pseudocheirus (Pseudocheirus) archeri</i>	Green Ringtail Possum	Q	45.1	0.52	0.51	0.68	0.19	60.64*	5.87	0.59	1.01	0.35* ¹	–	–
Vombatidae	<i>Vombatus ursinus</i>	Common Wombat	Q	137.7	0.37	0.43	0.60	0.19	55.58	59	0.38	0.85	0.54	–	–
Primates															
Cheirogaleidae															
	<i>Cheirogaleus medius</i>	Fat-tailed Dwarf Lemur	NO	33.3	0.57	0.60	0.63	0.22	44.86	2.6 [±]	0.79	1.06	1.24	–	–
	<i>Microcebus rufus</i>	Red Mouse Lemur	NO	23.1	0.51	0.53	0.56	0.20	27.85	1.72 [±]	1.01	1.36	1.92* ²	–	–
Daubentoniidae															
	<i>Daubentonia madagascariensis</i>	Aye-aye	NO	68.0	0.52	0.49	0.62	–	36.23	44.85 [±]	1.18	1.66	2.16	–	–
Galagonidae															
	<i>Galago alleni</i>	Bioko Allen's Bushbaby	O	39.3	0.48	0.47	0.48	0.17	–	5.85	0.93	1.24	1.65* ³	–	–
	<i>Galago demidovii</i>	Demidoff's Bushbaby	NO	29.3	0.50	0.49	0.51	0.19	17.55	2.65 [±]	1.06	1.41	2.28	–	–
	<i>Galago matschiei</i>	Dusky Bushbaby	O	34.9	0.51	0.46	0.48	0.16	–	4.62 [±]	1.14	1.40	1.59* ²	–	–
	<i>Galago senegalensis</i>	Senegal Bushbaby	O	32.0	0.48	0.44	0.48	0.15	16.73	3.96 [±]	1.12	1.38	1.49	–	–
	<i>Otolemur crassicaudatus</i>	Brown Greater Galago	NO	54.1	0.54	0.53	0.56	0.20	27.3	11.78 [±]	0.85	1.14	1.14* ²	–	–
Hominidae															
	<i>Gorilla beringei</i>	Mountain Gorilla	NB	–	–	–	–	–	16.25	–	–	–	–	11.54	10.62
	<i>Gorilla gorilla</i>	Western Gorilla	NB	202.4	0.39	0.47	0.54	0.17	30.91	–	–	–	–	11.12	9.50
	<i>Homo sapiens</i>	Human	B	156.0	0.29	0.32	0.41	0.13	–5.26	–	–	–	–	12.56	28.64
	<i>Pan troglodytes</i>	Chimpanzee	NB	151.0	0.39	0.46	0.54	0.19	19.27	–	–	–	–	8.60	12.04
	<i>Pongo abelii</i>	Sumatran Orangutan	NB	–	–	–	–	–	33.81	–	–	–	–	9.13	11.38
	<i>Pongo pygmaeus</i>	Bornean Orangutan	NB	177.5	0.42	0.48	0.53	0.17	33.01	–	–	–	–	10.15	11.26
Hylobatidae															
	<i>Bunopithecus hoolock</i>	Hoolock Gibbon	NB	–	–	–	–	–	32.42	–	–	–	–	13.78	7.58
	<i>Hylobates agilis</i>	Agile Gibbon	NB	–	–	–	–	–	23.90	–	–	–	–	7.34	11.91
	<i>Hylobates klossi</i>	Kloss's Gibbon	NB	–	–	–	–	–	27.20	–	–	–	–	7.69	10.94
	<i>Hylobates lar</i>	Lar Gibbon	NB	80.3	0.41	0.45	0.54	0.19	25.85	–	–	–	–	8.66	9.51
	<i>Hylobates muelleri</i>	Müller's Bornean Gibbon	NB	–	–	–	–	–	25.20	–	–	–	–	7.87	10.34
	<i>Hylobates pileatus</i>	Pileated Gibbon	NB	–	–	–	–	–	23.67	–	–	–	–	8.63	9.61
	<i>Nomascus (Hylobates) concolor</i>	Concolor Gibbon	NB	84.7	0.41	0.45	0.53	0.19	–	–	–	–	–	–	–
	<i>Symphalangus syndactylus</i>	Siamang	NB	–	–	–	–	–	34.78	–	–	–	–	8.25	9.09
Indridae															
	<i>Avahi laniger</i>	Eastern Woolly Lemur	O	39.9	0.58	0.49	0.61	–	28.99	9.86 [±]	1.18	1.51	0.9	–	–
	<i>Propithecus verreauxi</i>	Verreaux's Sifaka	O	61.4	0.52	0.48	0.56	0.21	26.07	26.21 [±]	1.00	1.31	1.09	–	–
Lemuridae															
	<i>Hapalemur griseus</i>	Lesser Bamboo Lemur	O	49.0	0.52	0.47	0.55	–	35.49	14.09 [±]	0.93	1.34	1.95* ²	–	–
	<i>Lemur catta</i>	Ring-tailed Lemur	NO	61.1	0.58	0.51	0.54	0.23	37.5	22.9 [±]	0.85	1.28	1.29	–	–

	<i>Lepilemur mustelinus</i>	Weasel Sportive Lemur	O	40.2	0.58	0.48	0.52	0.22	33.53	9.56 [±]	0.97	1.37	1.23 ^{*2}	–	–
	<i>Varecia variegata</i>	Ruffed Lemur	NO	73.4	0.59	0.56	0.56	0.23	41.63	32.12 [±]	0.69	1.02	1.53	–	–
Lorisidae	<i>Arctocebus calabarensis</i>	Angwantibo	NO	38.1	0.63	0.62	0.66	0.23	–	6.92 [±]	1.01	1.39	1.78 ^{*2}	–	–
	<i>Loris tardigradus</i>	Slender Loris	NO	34.7	0.53	0.58	0.63	0.21	14.44	5.87 [±]	1.03	1.50	1.44	–	–
	<i>Nycticebus coucang</i>	Slow Loris	NO	49.4	0.61	0.58	0.64	0.24	34.4	10.13 [±]	0.97	1.27	1.8	–	–
<u>Rodentia</u>															
Anomaluridae	<i>Anomalurus derbianus</i>	Lord Derby's Scaly-tailed Squirrel	Q	43.77	0.51	0.48	0.77	0.21	–	–	–	–	–	–	–
	<i>Anomalurus jacksonii</i>		Q	43.77	0.52	0.48	0.77	0.23	–	–	–	–	–	–	–
	<i>Anomalurus pelii</i>	Pel's flying Squirrel	Q	56.44	0.52	0.48	0.76	0.23	–	–	–	–	–	–	–
	<i>Anomalurus pusillus</i>	Dwarf scaly-tailed Squirrel	Q	36.32	0.51	0.47	0.76	0.21	–	–	–	–	–	–	–
Dipodidae	<i>Allactaga elater</i>	Five-toed Jerboa	B	23.6	0.30	0.39	0.63	0.21	47.35 [*]	1.16 ⁺	0.62	1.42	1.26 ^{*1}	–	–
	<i>Dipus sagitta</i>	Northern Three-toed Jerboa	B	25.9	0.35	0.45	0.69	0.21	50.33	1.28 [*]	0.56	1.27	0.96 ^{*1}	–	–
	<i>Eozapus setchuanus</i>	Chinese Jumping Mouse	B	16.4	0.49	0.50	0.75	0.22	–	–	–	–	–	–	–
	<i>Jaculus jaculus</i>	Lesser Egyptian Jerboa	B	22.9	0.38	0.46	0.74	0.19	43.31	1.48 ⁺	0.67	1.56	1.46	–	–
	<i>Napaeozapus insignis</i>	Woodland Jumping Mouse	Q	16.3	0.53	0.50	0.77	0.24	49.66	0.46 ⁺	0.65	1.38	0.82	–	–
	<i>Sicista betulina</i>	Northern Birch Mouse	Q	13.6	0.47	0.53	0.77	0.26	–	–	–	–	–	–	–
	<i>Sicista concolor</i>	Chinese Birch Mouse	Q	13.4	0.48	0.49	0.72	–	–	–	–	–	–	–	–
	<i>Sicista</i> sp.	Birch Mouse	Q	12.4	0.47	0.51	0.75	0.25	–	–	–	–	–	–	–
	<i>Zapus hudsonicus</i>	Meadow Jumping Mouse	Q	15.6	0.53	0.51	0.79	0.23	–	0.53 ⁺	0.73	1.47	1.16	–	–
Heteromyidae	<i>Chaetodipus hispidus</i>	Hipsid Pocket Mouse	Q	20.3	0.46	0.50	0.74	0.24	64.22	0.66 [#]	0.53	1.21	0.82	–	–
	<i>Chaetodipus intermedius</i>	Rock Pocket Mouse	Q	16.2	0.43	0.45	0.67	0.20	–	–	–	–	–	–	–
	<i>Chaetodipus penicillatus</i>	Desert Pocket Mouse	Q	17.3	0.45	0.48	0.70	0.22	52.37	0.44 [#]	0.60	1.25	1.03	–	–
	<i>Dipodomys deserti</i>	Desert Kangaroo Rat	B	30.2	0.42	0.43	0.60	0.19	42.14	1.68 [#]	0.68	1.48	0.86	–	–
	<i>Dipodomys merriami</i>	Merriam's Kangaroo Rat	B	23.9	0.46	0.46	0.61	0.20	47.7	1.11 [#]	0.69	1.29	1.27	–	–
	<i>Dipodomys ordii</i>	Ord's Kangaroo Rat	B	25.6	0.44	0.45	0.64	0.21	53.78	1.46 [#]	0.64	1.32	1.26	–	–
	<i>Dipodomys spectabilis</i>	Banner-tailed Kangaroo Rat	B	31.6	0.42	0.43	0.60	0.21	52.5	2.08 [#]	0.63	1.39	0.84	–	–
	<i>Heteromys gaumeri</i>	Gaumer's Spiny Pocket Mouse	Q	21.2	0.46	0.50	0.71	0.24	52.74 [*]	0.89 ⁺	0.59	1.57	1.01 ^{*4}	–	–
	<i>Liomys salvini</i>	Spiny Pocket Mouse	Q	20.0	0.45	0.51	0.74	0.25	43.83	0.74 ⁺	0.55	1.39	0.8	–	–
Muridae	<i>Gerbillus (Dipodillus) campestris</i>	North African Gerbil	Q	21.2	0.42	0.51	0.77	0.20	–	0.87 ⁺	0.57	1.28	1.36	–	–
	<i>Gerbillus dasyurus</i>	Wagner's Gerbil	Q	19.6	0.39	0.49	0.75	0.20	50.32	1.27 ⁺	0.75	1.70	2.48	–	–
	<i>Meriones persicus</i>	Persian Jird	Q	29.8	0.43	0.49	0.72	0.21	–	–	–	–	–	–	–
	<i>Psammomys obesus</i>	Fat Sand Rat	Q	29.7	0.43	0.46	0.77	0.21	–	–	–	–	–	–	–
	<i>Tatera brantsi</i>	Large Naked-soled Gerbils	Q	26.3	0.46	0.52	0.77	0.21	–	1.51 ⁺	0.57	1.36	0.96	–	–
Pedetidae	<i>Pedetes capensis</i>	Springhare/Springhaas	B	66.39	0.47	0.37	0.81	0.16	–	–	–	–	–	–	–
	<i>Pedetes surdaster</i>	East African Springhare	B	66.79	0.45	0.36	0.77	0.15	–	–	–	–	–	–	–

Legend: L = locomotion; P = posture; Q = quadruped; B = biped; NO = non-orthograde; O = orthograde; NB = non-biped; FMA = species mean foramen magnum angle (i.e., orientation); ECV = species mean endocranial volume; B/PL = species mean cubed root of brain volume divided by palate length; B/PLW = species mean cubed root of brain volume divided by the geometric mean of palate length and width; EQ = encephalization quotient; BI = species mean bicarotid index; WI = species mean Weidenreich index.

^a Foramen magnum angle measurements obtained from [Ruth et al. \(2016\)](#) where possible and subtracted from 180. Asterisk where FMA was measured by G.A.R. and E.C.K. for this study.

^b EQ value taken from [Boddy et al., 2012](#) where possible. Asterisk where EQ is calculated using the mammal equation provided by [Boddy et al., 2012](#) (see Methods) for this study; ^{*1} = body mass for calculation taken from [Silva and Downing \(1995\)](#); ^{*2} = body mass for calculation taken from [Isler et al. \(2008\)](#); ^{*3} = body mass for calculation taken from [Smith and Jungers \(1997\)](#); ^{*4} = body mass for calculation taken from [Nowak \(1999\)](#).

^{*} FMA or EQ measurement taken by G.A.R. and E.C.K. for this study.

⁻ ECV from [Ashwell \(2008\)](#).

[±] ECV from [Isler et al. \(2008\)](#).

⁺ ECV back-calculated from EQ.

[#] [Hafner and Hafner \(1984\)](#).

Table 2
Study variables, descriptions, calculations, and list of relevant citations. See Materials and methods (2.2 Data collection) for additional detail on metric calculations. See also Figure 1 in the present study and Figure 1 in Russo and Kirk (2013).

Variable	Description	Calculation	References
Foramen magnum angle	Measure of the anteroposterior inclination of the opening of foramen magnum	Angle between a chord connecting basion and opisthion, and the Frankfort Horizontal plane	Ruth et al. (2016)
Encephalization quotient	The difference between a species' observed brain size and the brain size expected for its body size	Data taken from Boddy et al. (2012). For taxa included in their study: brain mass/0.056 × body mass ^{0.746}	Boddy et al. (2012)
Molar ratio	The anteroposterior position of basion relative to the distalmost molar; a measure of foramen magnum position (FMP)	Average distance from the distalmost aspects of the left and right molars to a basion reference plane, divided by the geometric mean of cranial length and width (cranial size)	Russo and Kirk (2013)
Palate ratio	The anteroposterior position of basion relative to the posteriormost aspect of the bony palate at midline; measure of FMP	Distance from the posteriormost aspect of the bony palate at midline to basion, divided by cranial size	Russo and Kirk (2013)
Temporal fossa ratio	The anteroposterior position of basion relative to the anteriormost aspect of the temporal fossa; measure of FMP	Average distance from the anteriormost aspects of the left and right temporal fossae to a basion reference plane, divided by cranial size	Russo and Kirk (2013)
Basioccipital ratio	The anteroposterior position of basion relative to the spheno-occipital synchondrosis; measure of FMP	Distance from the spheno-occipital synchondrosis at midline (i.e., sphenobasion) to basion, divided by cranial size	This study
Cube root of endocranial volume (ECV)/palate length	Neocortex size relative to the size of the masticatory apparatus (here, palate length)	Cube root of ECV divided by the linear distance from prosthion to staphylion	Ross and Ravosa (1993)
Cube root of ECV/geomean of palate length and width	Neocortex size relative to the size of the masticatory apparatus (here, palate length and width)	Cube root of ECV divided by the geometric mean of 1) the linear distance from prosthion to staphylion and 2) the maximum transverse distance across the bony palate to the lingualmost surface of the cheek teeth	This study

incorporating quantitative data on masticatory apparatus size, and by examining measures of both FMP and FMA (Table 2).

1.1.3. Objective #3 Our third objective was to identify additional mammalian clades for which FMP could be compared between bipeds and quadrupeds. Previously, we examined four clades in which bipedal locomotion evolved independently: hominoid primates, dipodid rodents, heteromyid rodents, and diprotodont marsupials. Each mammalian clade that has independently evolved bipedal locomotion provides an opportunity to test the hypothesized functional association between a forward shift in FMP and bipedalism. Accordingly, we quantified FMP in a third rodent clade – Anomaluroidea – that contains bipedal springhares (*Pedetes* spp.) and gliding/quadrupedal anomalures² (*Anomalurus* spp.) (Fabre et al., 2012, 2013) (Fig. 2; see also SOM Fig. S2). *Pedetes* (Pedetidae) includes two species (East African *Pedetes surdaster* and South African *Pedetes capensis*) of large-bodied (3 – 4 kg), terrestrial and nocturnal rodents with a preference for arid or semi-arid flat terrain having little vegetation and short grass cover, and sandy soils for burrowing (Butynski, 1984, 2013). Ecologically, bipedal *Pedetes* and bipedal dipodids and heteromyids occupy similar niches (Butynski and Mattingly, 1979; Butynski, 1984). These rodent groups also morphologically converge in having long, powerful hind limbs and short forelimbs, giving *Pedetes* a “kangaroo-like appearance” (Nowak, 1999:1621; see also Fig. 2C and D), and reflecting their primary use of ricochet bipedal saltation (though *Pedetes* may use its forelimbs during slow locomotor progression like some bipedal

macropodids) (Butynski and Mattingly, 1979; Butynski, 1984, 2013; Samuels and Van Valkenburgh, 2008). *Anomalurus* (Anomaluridae) includes multiple arboreal and nocturnal species that span a range of body sizes from about 0.3 g (*Anomalurus pusillus*) to 2 kg (*Anomalurus peli*) (Nowak, 1999). Like phalangers (*Petaurus*: Diprotodontia), all species of *Anomalurus* possess patagia between the forelimb, hind limb, and tail that are used to glide between widely spaced arboreal supports (Nowak, 1999). During progression along arboreal substrates, however, *Anomalurus* relies on quadrupedal walking, running, and climbing (Nowak, 1999). Morphologically, *Anomalurus* lacks the extreme disparity in forelimb to hind limb proportions seen in *Pedetes* (Nowak, 1999; Samuels and Van Valkenburgh, 2008), and its overall external appearance resembles true squirrels (Scuridae). Based on the results of our prior analyses (Russo and Kirk, 2013), we expect bipedal *Pedetes* to have a more anteriorly positioned foramen magnum than quadrupedal/gliding *Anomalurus*.

1.1.4. Objective #4 Our fourth objective was to test an assertion central to Ruth and colleagues' (2016:51) critique of our previous study (Russo and Kirk, 2013): that their FMA measurement is an “accurate representation of [foramen magnum] location, including [its] position along the anterior–posterior axis of the basicranium”. To do so, we first examined the relationship between FMA and standard measures of FMP using a large sample of extant hominoids ($n = 198$; Table 1; SOM Fig. S2). We then explored the relationship between FMA and our four metrics of FMP (Table 2) using the comparative mammalian sample of rodents, marsupials, and strepsirrhine primates included in our former study (Russo and Kirk, 2013; SOM Fig. S1). If FMA is an accurate representation of both the anteroposterior location and inclination of the foramen magnum, then FMA should predict some or all of the indices used to quantify only FMP.

² Here, we prefer the common name “anomalure” to “scaly-tailed squirrel” in order to avoid the inadvertent implication of a close relationship with sciurid rodents (Heritage et al., 2016).

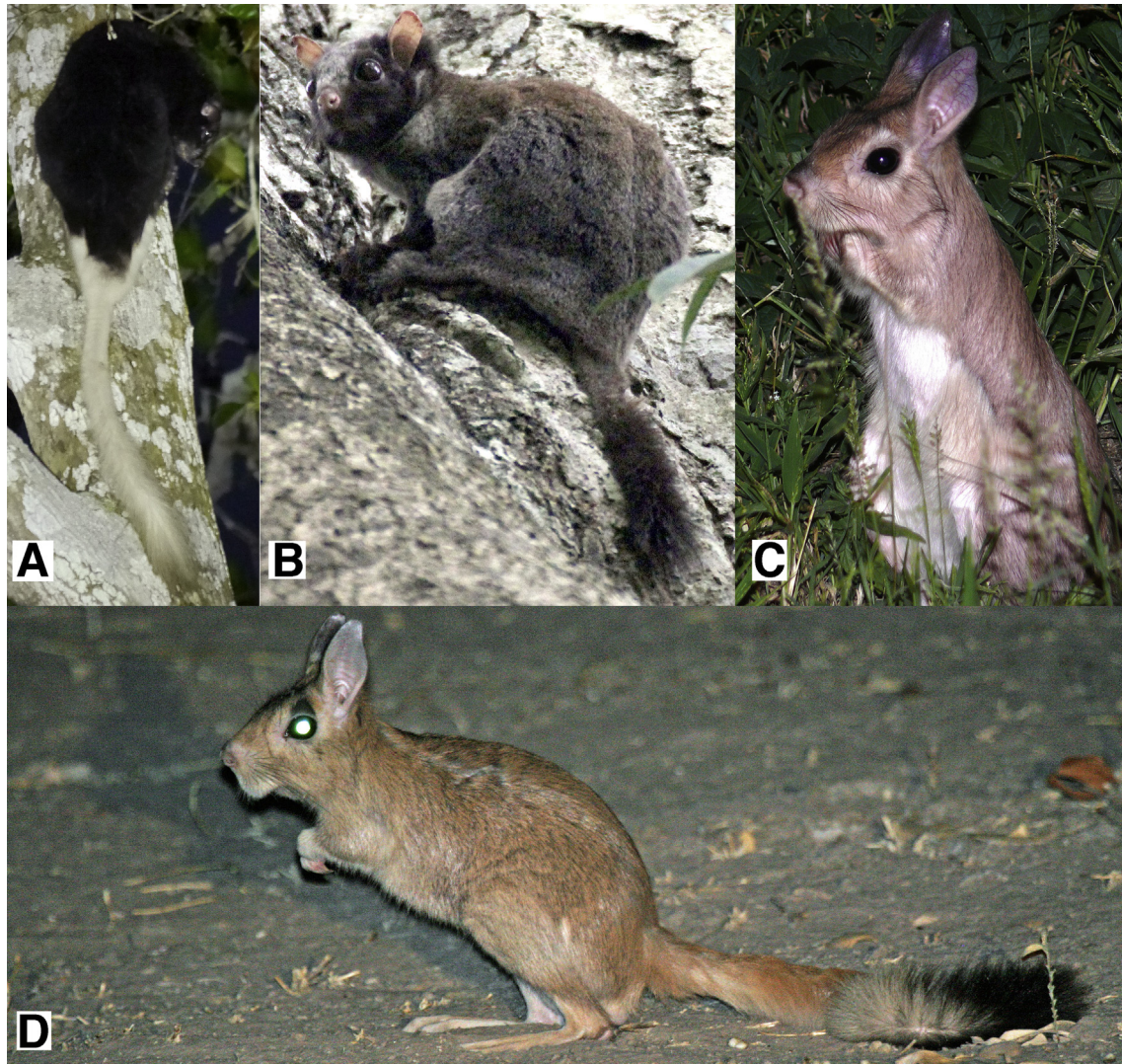


Figure 2. Examples of postures employed by anomaluroid rodents. A) *Anomalurus pelii*, courtesy of Nik Borrow; B) *Anomalurus derbianus*, courtesy of C. Smith and the American Society of Mammalogists Mammal Images Library; C) *Pedetes capensis*, courtesy of Bernard Dupont and Wikimedia Commons; D) *Pedetes capensis*, courtesy of B. D. Patterson and the American Society of Mammalogists Mammal Images Library.

2. Materials and methods

2.1. Sample

Data on molar ratio, palate ratio, temporal fossa ratio, and cranial size were taken from Russo and Kirk (2013) for 71 species of dipodid and heteromyid rodents, diprotodont marsupials, and strepsirrhine and hominoid primates (Table 1; SOM Fig. S2). Following Ruth et al. (2016), we classified *Galago demidovii* as ‘non-orthograde’, but all other locomotor and postural classifications in Russo and Kirk (2013) remain unchanged. Data were also collected for six species of anomaluroid rodents and 13 hominoid species (SOM Fig. S2) at the American Museum of Natural History (New York, NY, USA) and National Museum of Natural History (Washington, D.C., USA). The anomaluroid sample includes *P. capensis* ($n = 24$), *P. surdaster* ($n = 1$), *A. pelii* ($n = 4$), *A. jacksonii* ($n = 4$), *A. derbianus* ($n = 8$), and *A. pusillus* ($n = 8$) (total $n = 49$) (SOM Fig. S2). The expanded hominoid sample, collected as part of an ongoing study of basicranial morphological macroevolution across anthropoid primates (Russo et al., 2016), includes *Symphalangus symphalangus*

($n = 15$), *Bunopithecus (Hoolock) hoolock* ($n = 16$), *Hylobates agilis* ($n = 16$), *Hy. lar* ($n = 16$), *Hy. klossi* ($n = 16$), *Hy. muelleri* ($n = 16$), *Hy. pileatus* ($n = 10$), *Gorilla gorilla* ($n = 17$), *G. beringei* ($n = 15$), *Pongo pygmaeus* ($n = 17$), *Po. abelii* ($n = 12$), *Pan troglodytes* ($n = 13$), and *Homo sapiens* ($n = 16$) (total $n = 198$) (SOM Fig. S2). Museum specimen numbers for the entire sample included in the present study, as well as phylogenetic trees for the original study sample (SOM Fig. S1; Russo and Kirk, 2013) and the expanded mammal and hominoid sample (SOM Fig. S2) can be found in the Supplementary Online Material.

2.2. Data collection

Ratios expressing the position of basion relative to various basicranial landmarks were calculated from measurements taken on digital photographs of crania viewed in norma basilaris. Procedures for digital photography and photograph preparation (e.g., image rotation and scaling), and the linear measurements used to derive the molar ratio, palate ratio, and temporal fossa ratio, are described in Russo and Kirk (2013). We measured basioccipital length as the distance between sphenobasion and basion in all taxa

using NIH ImageJ software (Fig. 1). The speno-occipital synchondrosis was visible in many, but not all, adult specimens included in this analysis. When the speno-occipital synchondrosis was visible only at its lateral extents, a connecting line (using the ImageJ “line tool”) was drawn to approximate the position of the speno-occipital synchondrosis at the midline (i.e., sphenobasion). Assessments of sphenobasion position in specimens with partly fused speno-occipital synchondroses were confirmed by examining subadult specimens with unfused speno-occipital synchondroses. Specimens for which the speno-occipital synchondrosis could not be confidently identified were omitted from the sample. For each individual, a basioccipital ratio was calculated by dividing basioccipital length by the geometric mean of cranial length and width (“cranial size”, following Russo and Kirk, 2013).³

Encephalization quotients (EQs) were taken from Boddy et al. (2012; their Table S1) and are reported in Table 1. We calculated EQs for taxa (indicated in Table 1) not included in the study by Boddy et al. (2012) using the equation reported from their mammalian sample ($EQ = \text{brain mass} / 0.056 \times \text{body mass}^{0.746}$). For these taxa, brain masses were measured directly from museum specimens (see below) or calculated using reported endocranial volumes (ECV) as: $\text{brain mass} = ECV \times 1.036 \text{ g}$ (Isler et al., 2008). Body mass data were taken from the literature (Silva and Downing, 1995; Smith and Jungers, 1997; Nowak, 1999; Isler et al., 2008) (Table 1). EQ values > 1 indicate that the species' brain mass is larger than expected for its body size, whereas EQ values < 1 indicate that the species' brain is smaller than expected for its body size.

Measurements of ECV were obtained from the published literature for most species (Table 1) (Hafner and Hafner, 1984; Ashwell, 2008; Isler et al., 2008). For some taxa (indicated in Table 1), we calculated ECV by dividing brain masses reported in grams in Boddy et al. (2012) by 1.036 (see above). Where we could not obtain any published brain size data we took direct measurements of ECV from museum specimens (approximately six individuals per species; indicated in Table 1) using 3 mm glass beads. Prior to filling the braincase of a specimen with beads, cranial foramina were blocked with cotton. While filling the braincase, crania were gently agitated until beads were flush with the plane of the foramen magnum to ensure that the braincase was completely filled. The volume of glass beads was subsequently measured in 5, 10, or 25 mL graduated cylinders. We used ECV to calculate two measures of brain size relative to masticatory apparatus size. Following Ross and Ravosa (1993), we divided the cube root of ECV by palate length, measured as the linear distance between prosthion and staphylion (cm) (Table 2). Additionally, to account better for transverse dimensions of facial size (Bastir et al., 2010), we divided the cube root of ECV by the geometric mean of palate length and palate width (measured as the maximum transverse distance across the bony palate to the lingualmost surface of the cheek teeth [cm]) (Table 2). Measurements of palate length and width were obtained from digital photographs using ImageJ (Fig. 1).

To evaluate the relationship between FMP and FMA in the expanded hominoid dataset (Table 1; SOM Fig. S2), we quantified FMP using two metrics previously employed in the paleoanthropological literature. First, we quantified FMP as the linear distance between basion and the bicarotid chord (White et al.,

1994; Suwa et al., 2009). We size-adjusted this distance by cranial size (herein, the bicarotid index) following our previous methods (Russo and Kirk, 2013) (Table 2). Second, we quantified FMP as the distance from opisthion to the posteriormost extent of the cranial vault divided by cranial length (glabella to the posteriormost extent of the cranial vault) (herein, the “Weidenreich index”, sensu Weidenreich, 1943; Kimbel et al., 2004). Linear distances used to calculate these two measures of FMP were derived from 3D landmarks obtained on crania using a MicroScribe G2X digitizer (Revware Systems, Inc., Raleigh, NC, USA). Foramen magnum orientation for these specimens was measured in ImageJ from photographs of crania in norma lateralis as the angle between a chord aligned with the basion-opisthion plane (extended with a straight-edge ruler) and the Frankfort Horizontal (“FMA” in Fig. 1; see also SOM Fig. S3). We opted to measure the inclination of the basion-opisthion chord relative to the Frankfort Horizontal rather than the orbital plane (Strait and Ross, 1999) to maintain consistency with the paleoanthropological literature (e.g., Kimbel et al., 2004) and because Ruth et al. (2016) also used the Frankfort Horizontal as a reference line for marsupials and strepsirrhines. In this way, we were able to incorporate the data on FMA provided by Ruth et al. (2016) for analysis of FMA and FMP in an expanded mammalian sample. We also took photographs of crania in norma lateralis to collect measurements of FMA for mammalian taxa that were included in Russo and Kirk (2013) but not in Ruth et al. (2016) in an attempt to complete the data set. We were able to include FMA measurements for seven additional rodent and marsupial taxa (indicated in Table 1). Following Ruth et al. (2016), we used the occlusal plane and the Frankfort Horizontal as the reference lines for the basion – opisthion chord in rodents and marsupials, respectively. It should be noted that because our preferred method for measuring FMA follows that of Kimbel et al. (2004), we subtracted the FMA values obtained by Ruth et al. (2016) from 180 in order to make angular measurements comparable (Table 1).

2.3. Data analysis

Differences in species mean basioccipital ratios between bipedal/orthograde and quadrupedal/non-orthograde taxa were quantified using Mann–Whitney U tests following Russo and Kirk (2013) in SPSS v. 22.0 (IBM Corporation, 2013). Also following Russo and Kirk (2013), comparisons were made within higher taxa (i.e., Rodentia, Diprotodontia, Strepsirrhini, and Hominoidea) to minimize the influence of phylogenetic differences between the clades. Tests were one-tailed because we expected bipedal and orthograde groups to have lower ratios (associated with a forward translation of the foramen magnum and shortening of the basioccipital) compared to their quadrupedal or non-orthograde close relatives. Following our previous study (Russo and Kirk, 2013), we elected to analyze individuals for the hominoid analysis of basioccipital length to evaluate better the performance of our measures for distinguishing between modern humans and other hominoids. As with hominoids, it was necessary to evaluate individuals for the ratio comparisons within anomaluroids because the sample for this clade also included a small number of species ($n = 6$).

The relationship between species means of FMA and our four metrics of FMP (i.e., molar ratio, palate ratio, temporal fossa ratio, and basioccipital ratio) versus each metric of relative brain size (i.e., EQ, the cube root of ECV divided by palate length, and the cube root of ECV divided by the geometric mean of palate length and width) was examined using phylogenetic generalized least-squares (PGLS) regressions. We

³ Muchlinski (2010) examined the relationship between cranial size and body mass using a large comparative sample ($n = 4122$ specimens of >500 thierian species) and found a significant positive correlation between the two variables (Spearman's $r = 0.97$) and an RMA slope confidence interval that included isometry.

also used PGLS to examine the relationship between species means of our metrics of FMP (bicarotid index and Weidenreich index for hominoids; and the molar, palate, temporal fossa, and basioccipital ratios for rodents, marsupials, and strepsirrhines) and FMA. In this study, PGLS was used to account for more similar cranial morphologies among closely related taxa than distantly related taxa (Martins and Hansen, 1997). Phylogenetic tree topology and branch lengths follow Bininda-Emonds et al. (2007) for all taxa with the exception of the hominoids, for which we used Primate 10kTrees (version 3 with Wilson and Reeder (2005) taxonomy; Arnold et al., 2010) in order to include all of our sampled species. We evaluated relationships among FMA, FMP, and various metrics of relative brain size within each clade in order to evaluate how our results compare to the findings by Ruth et al. (2016) (who also performed analyses by clade), and because the method of measuring FMA for rodents differed slightly from that for marsupials, strepsirrhines, and hominoids (following Ruth et al., 2016). Prior to analysis, measures of FMA (in degrees) were transformed into radians and ratios were examined as quotients. PGLS analyses were conducted in R (R Core Team, 2014) using the ape and nlme packages (Paradis et al., 2004; Pinheiro et al., 2014).

3. Results

3.1. Objective #1: FMP as quantified by basioccipital ratio

Consistent with predictions, bipedal dipodid and heteromyid rodents, bipedal marsupials, and modern humans have significantly lower basioccipital ratios compared to their quadrupedal counterparts (rodents: $z = 2.048$, $p = 0.021$; marsupials: $z = 1.741$, $p = 0.044$; hominoids: $z = -5.538$, $p < 0.001$; Fig. 3). Also in accord with predictions, orthograde strepsirrhines have significantly lower basioccipital ratios compared to non-orthograde strepsirrhines ($z = 1.800$, $p = 0.042$; Fig. 3). While there is some overlap in the ranges between categories, these comparisons reveal that bipedal rodents, bipedal marsupials, modern humans, and orthograde strepsirrhines tend to have more shortened basioccipital segments and more anteriorly positioned foramina magna than their quadrupedal and non-orthograde close phyletic relatives.

3.2. Objective #2: effect of relative brain size on FMP and FMA

Consistent with the literature on expanded mammalian samples (Martins and Hansen, 1997), brain size has a negative allometric relationship with body size (RMA: $0.721[x] \pm 2.746$; Adjusted

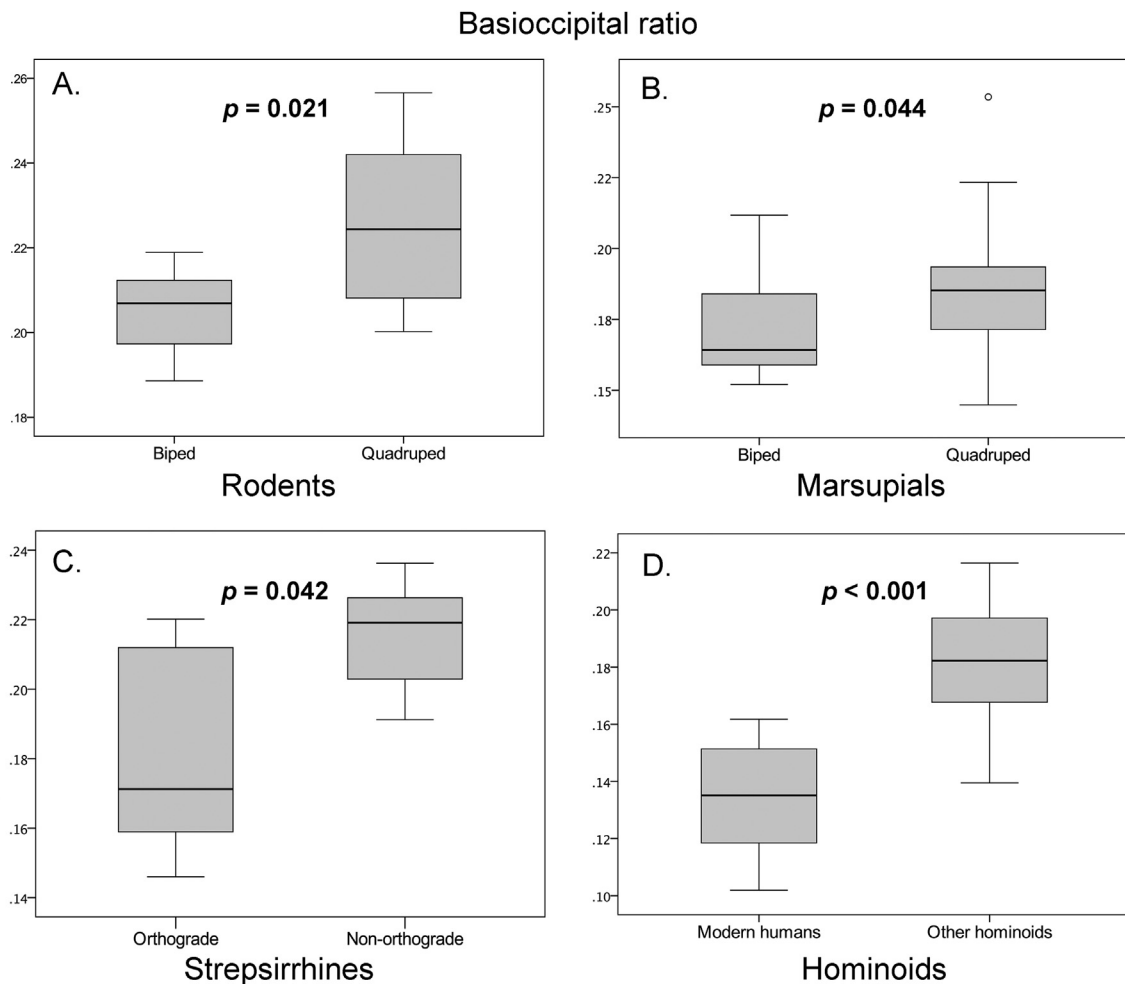


Figure 3. Basioccipital ratios for A) rodents [excluding anomaluroids, see Fig. 4], B) marsupials, C) strepsirrhines, and D) hominoids. Ratio values represent species means with the exception of hominoids, which are evaluated as individuals. Low values indicate that basioccipital length is relatively short, and high values indicate that basioccipital length is relatively long.

Table 3
Rodent PGLS regression results for analyses of foramen magnum angle, four metrics of foramen magnum position, and three metrics of relative brain size. Significant ($p < 0.05$) results in bold typeface.

Rodents					
Response Variable	Predictor Variable	slope	intercept	p-value	lambda
Foramen Magnum Angle	Encephalization Quotient	-0.185	1.076	0.230	0.000
Foramen Magnum Angle	Cube root of ECV/palate length	-1.370	1.723	0.003	0.162
Foramen Magnum Angle	Cube root of ECV/geomean of palate length and width	-0.500	1.577	0.036	0.000
Molar Ratio	Encephalization Quotient	-0.018	0.509	0.296	1.000
Molar Ratio	Cube root of ECV/palate length	-0.139	0.574	0.165	1.000
Molar Ratio	Cube root of ECV/geomean of palate length and width	-0.066	0.581	0.128	1.000
Molar Ratio	Foramen Magnum Angle	0.055	0.429	0.328	1.000
Palate Ratio	Encephalization Quotient	-0.031	0.471	0.271	1.000
Palate Ratio	Cube root of ECV/palate length	-0.037	0.458	0.824	1.000
Palate Ratio	Cube root of ECV/geomean of palate length and width	-0.065	0.525	0.371	1.000
Palate Ratio	Foramen Magnum Angle	-0.056	0.374	0.578	1.000
Temporal Fossa Ratio	Encephalization Quotient	-0.018	0.753	0.516	1.000
Temporal Fossa Ratio	Cube root of ECV/palate length	-0.216	0.866	0.170	1.000
Temporal Fossa Ratio	Cube root of ECV/geomean of palate length and width	-0.060	0.817	0.389	1.000
Temporal Fossa Ratio	Foramen Magnum Angle	0.165	0.588	0.122	1.000
Basioccipital Ratio	Encephalization Quotient	-0.011	0.230	0.265	0.880
Basioccipital Ratio	Cube root of ECV/palate length	-0.128	0.296	0.020	1.000
Basioccipital Ratio	Cube root of ECV/geomean of palate length and width	-0.047	0.282	0.058	1.000
Basioccipital Ratio	Foramen Magnum Angle	0.107	0.123	0.027	1.000

Table 4
Marsupial PGLS regression results for analyses of foramen magnum angle, four metrics of foramen magnum position, and three metrics of relative brain size.

Marsupials					
Response Variable	Predictor Variable	slope	intercept	p-value	lambda
Foramen Magnum Angle	Encephalization Quotient	-0.267	1.046	0.139	0.000
Foramen Magnum Angle	Cube root of ECV/palate length	-0.072	0.925	0.867	0.000
Foramen Magnum Angle	Cube root of ECV/geomean of palate length and width	-0.020	0.907	0.946	0.000
Molar Ratio	Encephalization Quotient	-0.016	0.514	0.719	0.960
Molar Ratio	Cube root of ECV/palate length	-0.114	0.561	0.260	1.000
Molar Ratio	Cube root of ECV/geomean of palate length and width	-0.070	0.567	0.326	1.000
Molar Ratio	Foramen Magnum Angle	-0.051	0.550	0.370	1.000
Palate Ratio	Encephalization Quotient	0.015	0.473	0.790	1.000
Palate Ratio	Cube root of ECV/palate length	0.158	0.402	0.155	1.000
Palate Ratio	Cube root of ECV/geomean of palate length and width	0.103	0.389	0.161	1.000
Palate Ratio	Foramen Magnum Angle	-0.046	0.531	0.426	1.000
Temporal Fossa Ratio	Encephalization Quotient	<0.001	0.653	0.995	0.747
Temporal Fossa Ratio	Cube root of ECV/palate length	0.141	0.582	0.277	0.714
Temporal Fossa Ratio	Cube root of ECV/geomean of palate length and width	0.071	0.590	0.433	0.743
Temporal Fossa Ratio	Foramen Magnum Angle	-0.010	0.666	0.894	0.847
Basioccipital Ratio	Encephalization Quotient	0.008	0.172	0.670	0.000
Basioccipital Ratio	Cube root of ECV/palate length	0.032	0.161	0.553	0.000
Basioccipital Ratio	Cube root of ECV/geomean of palate length and width	0.014	0.165	0.711	0.000
Basioccipital Ratio	Foramen Magnum Angle	0.007	0.178	0.837	0.000

$r^2 = 0.89$, $p < 0.001$) in the taxonomic sample specific to the studies of relevance here (Russo and Kirk, 2013; Ruth et al., 2016). As expected, this result indicates that ER (Ruth et al., 2016) tends to decrease with increasing body mass.

Results for the PGLS regressions of FMA and our four metrics of FMP versus (i.e., regressed against) three metrics of relative brain size (including EQ, the cube root of ECV divided by palate length and the cube root of ECV divided by the geometric mean of palate length and width) are presented below for rodents (Table 3; SOM Figs. S4–S8), marsupials (Table 4; SOM Figs. S9–S13), and strepsirrhine primates (Table 5; SOM Figs. S14–S18).

For rodents (Table 3; SOM Figs. S4–S8), results were non-significant ($p > 0.05$) for PGLS regressions of FMA and our four measures of FMP versus EQ. Results were also non-significant for regressions of three (molar, palate, and temporal fossa ratios) of our measures of FMP versus the cube root of ECV divided by palate length and the cube root of ECV divided by geometric mean of palate length and width. Results were significant ($p = 0.020$; Adjusted $r^2 = 0.28$) for the regression of basioccipital ratio versus the cube root of ECV divided by palate length, but this relationship

is non-significant once transverse dimensions of the masticatory apparatus are taken into account ($p = 0.058$). Results were also significant for the regression of FMA versus the cube root of ECV divided by palate length ($p = 0.003$; Adjusted $r^2 = 0.53$) and FMA versus the cube root of ECV divided by geometric mean of palate length and width ($p = 0.039$; Adjusted $r^2 = 0.28$).

For marsupials (Table 4; SOM Figs. S9–S13), results were non-significant ($p > 0.05$) for all analyses.

For strepsirrhines (Table 5; SOM Figs. S14–S18), results were non-significant ($p > 0.05$) for PGLS regressions of FMA and our four measures of FMP versus EQ. Regression results were significant for measures of FMA ($p = 0.025$; Adjusted $r^2 = 0.299$), the molar ratio ($p = 0.011$; Adjusted $r^2 = 0.316$), and the basioccipital ratio ($p = 0.016$; Adjusted $r^2 = 0.347$) versus the cube root of ECV divided by palate length. Measures of FMA generally decreased (i.e., the foramen magnum tilts more anteroinferiorly), and molar and basioccipital ratios decreased (i.e., the foramen magnum becomes more anteriorly positioned), as brain size relative to palate length increases. Once transverse dimensions of the masticatory apparatus are taken into account, this relationship was non-significant

Table 5

Strepsirrhine PGLS regression results for analyses of foramen magnum angle, four metrics of foramen magnum position, and three metrics of relative brain size. Significant ($p < 0.05$) results in bold typeface.

Strepsirrhines					
Response Variable	Predictor Variable	slope	intercept	<i>p</i> -value	lambda
Foramen Magnum Angle	Encephalization Quotient	−0.029	0.559	0.749	0.697
Foramen Magnum Angle	Cube root of ECV/palate length	−0.560	1.063	0.025	0.798
Foramen Magnum Angle	Cube root of ECV/geomean of palate length and width	−0.444	1.108	0.021	1.000
Molar Ratio	Encephalization Quotient	−0.030	0.576	0.339	1.000
Molar Ratio	Cube root of ECV/palate length	−0.207	0.732	0.011	1.000
Molar Ratio	Cube root of ECV/geomean of palate length and width	−0.149	0.729	0.035	1.000
Molar Ratio	Foramen Magnum Angle	0.184	0.427	0.064	0.788
Palate Ratio	Encephalization Quotient	−0.043	0.620	0.105	1.000
Palate Ratio	Cube root of ECV/palate length	−0.106	0.655	0.196	0.729
Palate Ratio	Cube root of ECV/geomean of palate length and width	−0.092	0.675	0.157	0.948
Palate Ratio	Foramen Magnum Angle	0.151	0.465	0.019	0.000
Temporal Fossa Ratio	Encephalization Quotient	−0.020	0.611	0.549	1.000
Temporal Fossa Ratio	Cube root of ECV/palate length	−0.064	0.642	0.493	1.000
Temporal Fossa Ratio	Cube root of ECV/geomean of palate length and width	−0.023	0.610	0.772	1.000
Temporal Fossa Ratio	Foramen Magnum Angle	0.174	0.487	0.082	1.000
Basioccipital Ratio	Encephalization Quotient	−0.004	0.176	0.824	1.000
Basioccipital Ratio	Cube root of ECV/palate length	−0.114	0.319	0.016	1.000
Basioccipital Ratio	Cube root of ECV/geomean of palate length and width	−0.064	0.294	0.157	0.941
Basioccipital Ratio	Foramen Magnum Angle	0.095	0.160	0.020	0.000

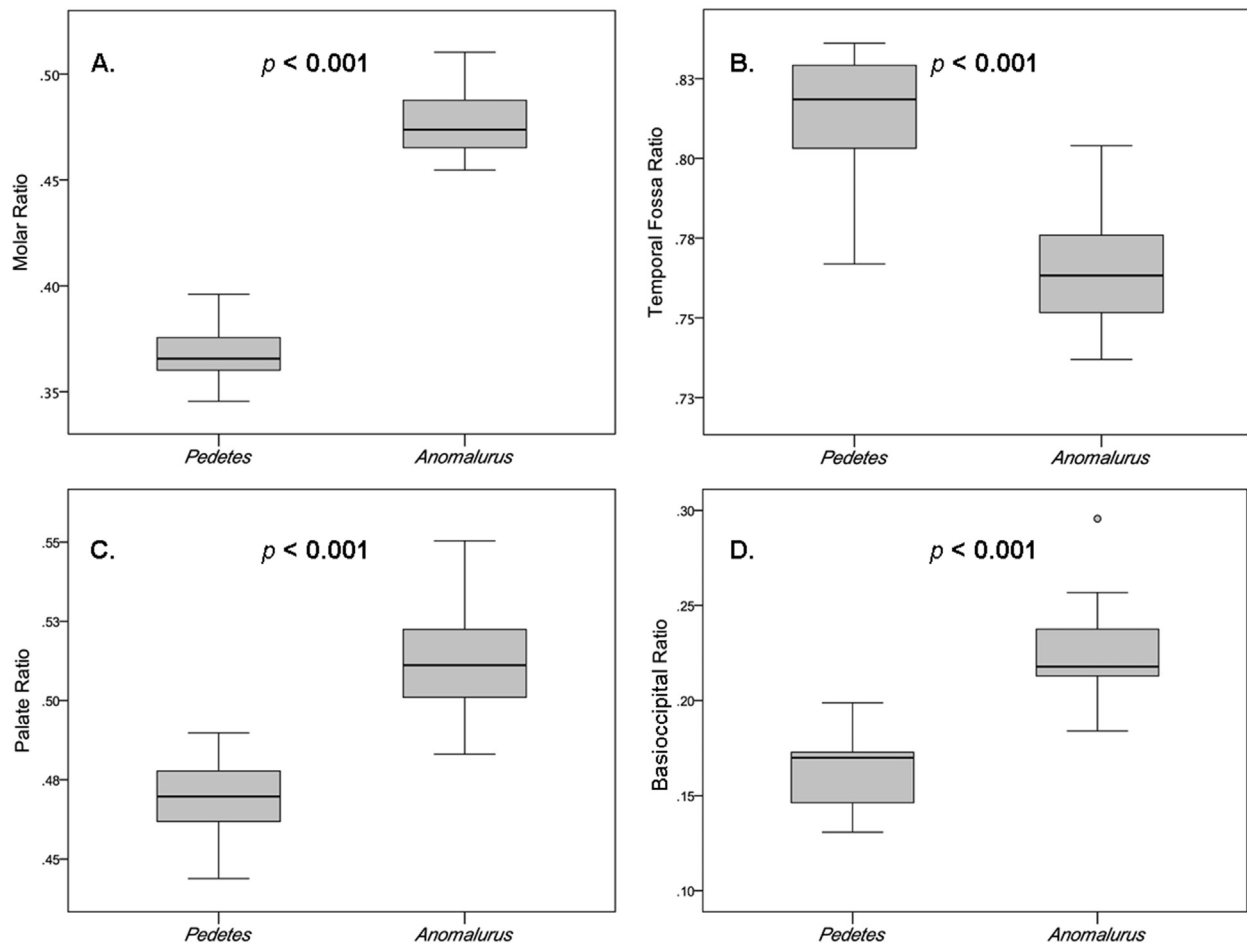


Figure 4. Molar ratio (A), temporal fossa ratio (B), palate ratio (C), and basioccipital ratio (D) for the anomaluroid sample evaluated using individuals. For panels A–C, low values indicate that the foramen magnum is relatively more anteriorly positioned and high values indicate that the foramen magnum is more posteriorly positioned. For panel D, low values specifically indicate that basioccipital length is relatively short and high values indicate that basioccipital length is relatively long.

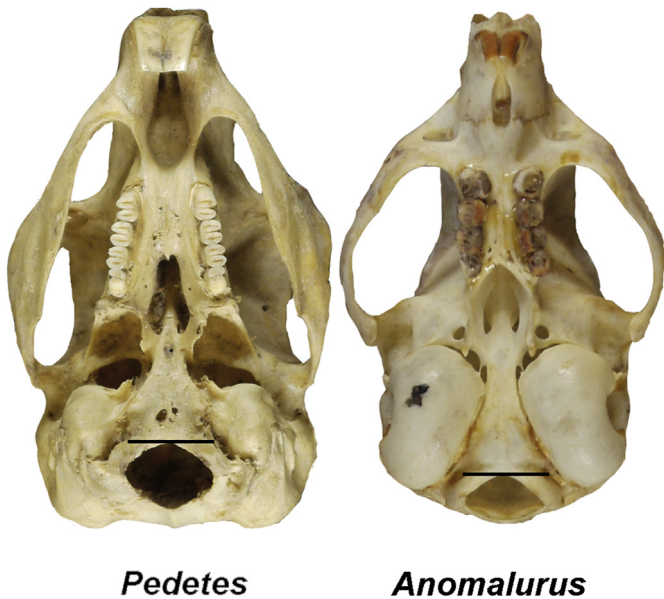


Figure 5. Representative crania of *Pedetes* and *Anomalurus* scaled to the same approximate length, with solid lines indicating basion position. See text for more details.

for the basioccipital ratio, but remained significant for FMA ($p = 0.021$; Adjusted $r^2 = 0.317$) and the molar ratio ($p = 0.035$; Adjusted $r^2 = 0.216$).

3.3. Objective #3: FMP in anomaluroid rodents

Figure 4 shows the molar ratio (Fig. 4A), temporal fossa ratio (Fig. 4B), palate ratio (Fig. 4C), and basioccipital ratio (Fig. 4D) for the anomaluroid sample, and Figure 5 shows a side-by-side comparison of representative crania of *Pedetes* and *Anomalurus*. *Pedetes* had significantly lower indices than *Anomalurus* for three of the ratios quantifying FMP (palate ratio: $z = 5.860$, $p < 0.001$; molar ratio: $z = 6.000$, $p < 0.001$; basioccipital ratio: $z = 5.123$, $p < 0.001$) (Fig. 4). Contrary to predictions, *Pedetes* had significantly higher temporal fossa ratios than *Anomalurus* ($z = -5.540$, $p < 0.001$) (Fig. 4). These results indicate that basion is more anteriorly positioned in bipedal *Pedetes* than in gliding/quadrupedal *Anomalurus* when basion is measured relative to the posterior molar, posterior palate, and spheno-occipital synchondrosis, but not when basion is measured relative to the anterior temporal fossa.

3.4. Objective #4: relationship between FMP and FMA

Table 6 and Figure 6 show the PGLS regression results of two standard measures of FMP versus FMA among hominoid individuals, with separate regressions for the sample including and

excluding *H. sapiens*. Regression results are non-significant ($p > 0.05$), with the exception of the Weidenreich index when *H. sapiens* is included in the sample ($p < 0.001$; Adjusted $R^2 = 0.75$). For this analysis, the Weidenreich index decreases (i.e., the foramen magnum becomes more posteriorly positioned) as FMA increases (i.e., the foramen magnum faces more posteriorly). However, the inclusion of *H. sapiens* largely drives this relationship among hominoids, as the relationship is non-significant ($p > 0.05$) with *H. sapiens* omitted from the sample.

Results for the PGLS regressions of our four measures of FMP versus FMA are presented below for rodents (Table 3, SOM Figs. S5–S8), marsupials (Table 4, SOM Figs. S10–S13), and strepsirrhine primates (Table 5, SOM Figs. S15–S18). Among rodents, results are non-significant ($p > 0.05$) with the exception of the basioccipital ratio versus FMA ($p = 0.027$; Adjusted $r^2 = 0.318$), for which increasing basioccipital ratio values (i.e., increasing basioccipital length) are associated with increasing FMA values (i.e., more posteriorly facing foramina magna). Among marsupials, results are non-significant for all analyses ($p > 0.05$). Among strepsirrhines, results are non-significant for the molar and temporal fossa ratios ($p > 0.05$), but are significant for analyses of the palate ratio ($p = 0.019$; Adjusted $r^2 = 0.326$) and the basioccipital ratio ($p = 0.020$; Adjusted $r^2 = 0.414$). For these analyses, increasing basioccipital and palate ratios are associated with increasing measures of FMA, indicating that increasing basioccipital segment lengths and increasingly posterior basion positions relative to the bony palate are both associated with a more posteriorly facing foramen magnum.

4. Discussion

In our original analysis of foramen magnum position (FMP) in mammals (Russo and Kirk, 2013), we examined four clades in which bipedal locomotion independently evolved: diprotodont marsupials, heteromyid rodents, dipodid rodents, and hominoid primates. To assess the possible influence of orthograde posture on FMP rather than bipedal locomotion per se (Kimbel and Rak, 2010), we also quantified FMP in strepsirrhine primates, which employ quadrupedal forms of locomotion but demonstrate considerable interspecific variation in trunk posture (see Table 1 in Russo and Kirk [2013] and citations therein). This paradigm relies on the comparative method (Harvey and Pagel, 1991; Coddington, 1994), in which instances of homoplasy are used to test hypothetical evolutionary associations. In the case of FMP, it is generally accepted that hominins have a more anteriorly positioned foramen magnum than do other primates (e.g., Daubenton, 1764; Topinard, 1890; Schultz, 1942, 1955; Luboga and Wood, 1990; Schaefer, 1999; Ahern, 2005; Russo and Kirk, 2013). However, the cause of this forward migration is the subject of greater debate, with researchers proposing multiple potential explanatory factors (e.g., locomotion, trunk and/or head posture, brain expansion and/or reorganization; e.g., Biegert, 1957, 1963; Kimbel and Rak, 2010; Ruth et al., 2016). Because the ultimate goal of our prior study (Russo and Kirk, 2013) was to

Table 6
Hominoid PGLS regression results for standard measures of foramen magnum position versus foramen magnum angle. Significant ($p < 0.05$) results in bold typeface. See also Fig. 6.

Hominoids						
Sample	Response Variable	Predictor Variable	slope	intercept	<i>p</i> -value	lambda
Including <i>H. sapiens</i>	Bicarotid index	Foramen Magnum Angle	−1.879	11.173	0.305	1.000
Excluding <i>H. sapiens</i>	Bicarotid index	Foramen Magnum Angle	−0.782	10.414	0.684	1.000
Including <i>H. sapiens</i>	Weidenreich index	Foramen Magnum Angle	−22.6303	21.998	<0.001	0.550
Excluding <i>H. sapiens</i>	Weidenreich index	Foramen Magnum Angle	−5.226	12.835	0.079	1.000

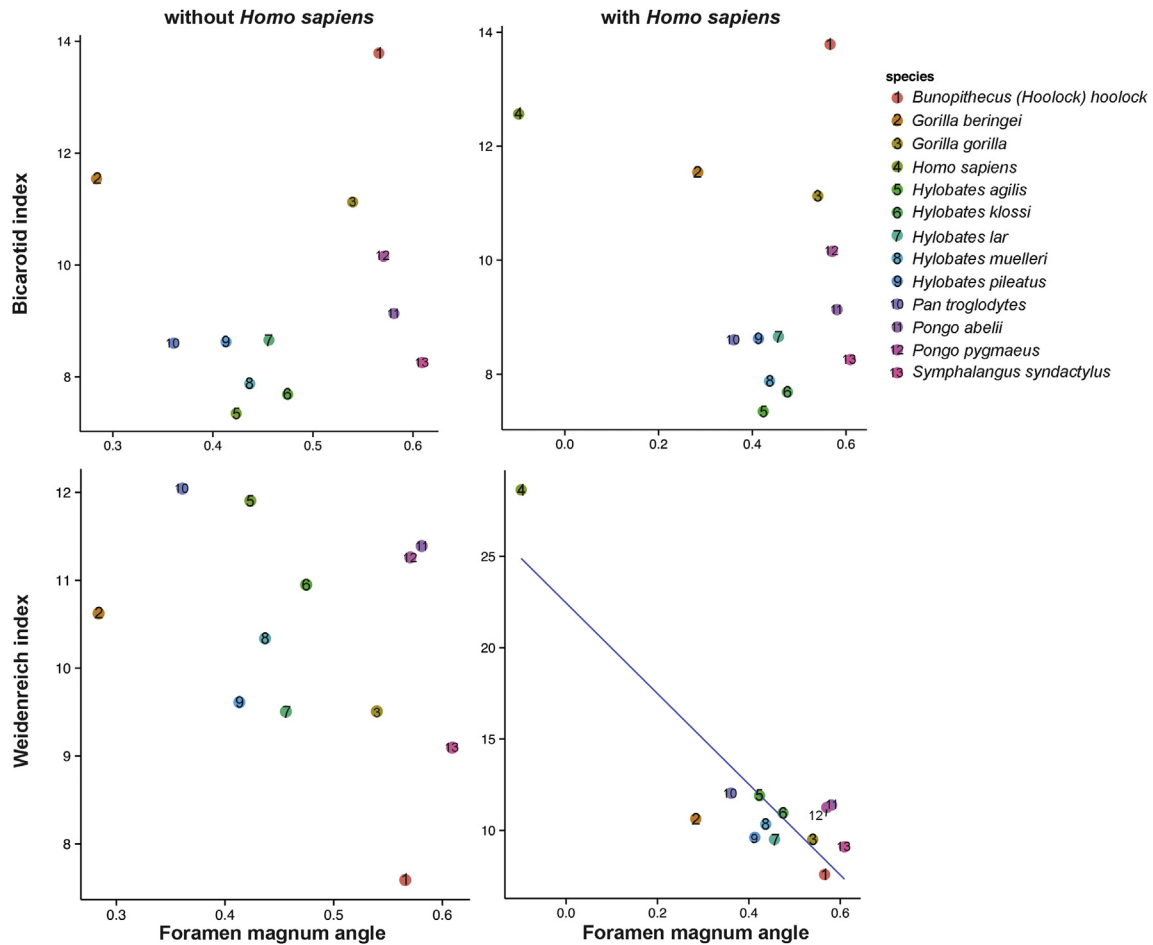


Figure 6. Bicarotid index (first row) and Weidenreich index (second row) versus foramen magnum angle in the hominoid sample (Table 1; SOM Fig. S2), excluding (first column) and including (second column) *Homo sapiens*. PGLS regression results are presented in Table 6.

determine if the anteriorly positioned foramina magna of some early fossil hominins (e.g., *Ardipithecus* and *Sahelanthropus*) could be attributed to bipedal locomotion, we employed the comparative method to determine if there was an association between anteriorly positioned foramina magna and bipedal locomotion across several distantly related mammalian lineages.

Analyses of FMP in hominoids have traditionally used a series of basicranial landmarks (e.g., bicarotid chord) as a fixed frame of reference for quantifying the relative position of basion (e.g., Schultz, 1942; Luboga and Wood, 1990; White et al., 1994; Schaefer, 1999; Ahern, 2005). Because these landmarks are not consistently visible in bipedal marsupials or rodents, we quantified basion position in our previous study using osteological landmarks that could be readily compared among mammalian taxa with disparate cranial morphologies (Russo and Kirk, 2013). These reference points included the anterior margin of the temporal fossa, the posterior aspect of the hard palate at midline, and the posterior aspect of the last adult molar crown. To compare FMP across a range of body sizes, we divided the linear distance between basion and each landmark by the geometric mean of cranial length and width (i.e., “cranial size”; Russo and Kirk, 2013). Regardless of which reference landmark was employed, our metrics showed that the foramen magnum was significantly more anteriorly positioned in bipedal marsupials, rodents, and hominoids than in their quadrupedal close relatives (Russo and Kirk, 2013). We also found that orthograde strepsirrhines had more anteriorly positioned foramina magna than non-orthograde strepsirrhines (Russo and Kirk, 2013), suggesting that

both bipedalism and orthograde trunk postures could potentially select for more anteriorly positioned foramina magna.

Ruth et al. (2016) reconsidered the metrics used in our initial analysis (Russo and Kirk, 2013) and concluded that the results for each of the non-hominoid clades that we examined could not be attributed to bipedalism or orthograde trunk posture, but were instead the result of confounding variables that we did not consider. According to Ruth et al. (2016), these variables include the size and position of the masticatory apparatus in marsupials, the size of the auditory bulla in rodents, and relative brain size in strepsirrhine primates. In other words, Ruth et al. (2016) assert that our results (Russo and Kirk, 2013) are attributable to different anatomical variables unrelated to bipedalism in each of the three non-hominoid groups that we examined. We find the claims of Ruth et al. (2016) to be unpersuasive for a variety of reasons, which we discuss in turn below in the context of the underlying theory and practical application of the comparative method, as well as the new findings from the four analyses (Objectives #1–4) presented in the current study.

4.1. Theory and practical application of the comparative method

Ruth et al. (2016) draw conclusions about the utility of the metrics employed in our previous study (Russo and Kirk, 2013) based on a qualitative assessment of limited comparative evidence. Ruth and colleagues state that they “demonstrate ... that the measurements used in [Russo and Kirk 2013] do not accurately correspond to FM position, but instead with the relative position and size

of the masticatory apparatus” (Ruth et al., 2016: 46). There are a number of key problems with this statement. First, Ruth et al. (2016) quantify neither the position of the foramen magnum nor the relative position and/or size of the masticatory apparatus in their analysis. In place of quantitative analyses, Ruth and colleagues rely on the untested assumption that their metric of foramen magnum angle (FMA) “accurately reflects both FM position and orientation” (Ruth et al., 2016: 47; see also below). This assertion is based on “a side-by-side comparison of species with the highest and lowest FMAs” (Ruth et al., 2016: 46–47) illustrated by photographs of two species: the pygmy rock wallaby (*Petrogale concinna*) and the swamp wallaby (*Wallabia bicolor*) (their Fig. 1B). Second, the conclusion that the metrics employed by us (Russo and Kirk, 2013) do not reflect FMP appears to be similarly based on qualitative visual inspection of only three species: the koala (*Phascolarctos cinereus*), the common wombat (*Vombatus ursinus*), and the crescent nail-tail wallaby (*Onychogalea lunata*) (Ruth et al., 2016, their Fig. 1A). In referring to these species, Ruth et al. (2016) present subjective conclusions about FMP, stating, for example, that the metrics used by Russo and Kirk (2013) “obviously reflect the positioning of the masticatory apparatus” (Ruth et al., 2016: 46) or “clearly reflect the position of the masticatory apparatus and not that of the [foramen magnum]” (Ruth et al., 2016: 48). Because Ruth et al. (2016) do not specify a fixed frame of reference by which FMP should be assessed (or quantified), we submit that these claims are neither clear nor obvious. Additionally, it may be considered axiomatic that comparative tests of evolutionary hypotheses are more convincing when they are based on large numbers of species. As expressed by Coddington (1994: 54–55) in his essay on homoplasy and the study of adaptation, the power of the comparative method is in its “emphasis on statistical patterns”, at “remove from the biology of any given instance”. The assertion that the metrics of Russo and Kirk (2013) reflect masticatory morphology rather than FMP carries little weight because the sample size on which it is based is evidently $n = 3$ species (Ruth et al., 2016). We therefore regard the proposition by Ruth et al. (2016) that their qualitative examination of three species shows that our (Russo and Kirk, 2013) quantitative study of 71 species did not accurately measure FM position as implausible.

In this context, it is also worth noting that for any comparison in which two groups of species differ significantly in a metric but nevertheless have overlapping ranges for that metric, it will always be possible to selectively draw species from the two groups that (when compared) do not appear to support the proposed relationship between the metric and the ecological or functional variable used to divide the sample into groups. Such individual comparisons do not negate the legitimacy of any larger comparative relationship that may be demonstrated by the expanded sample. For instance, ample comparative evidence demonstrates that nocturnal birds have significantly larger corneas relative to eye size than do diurnal birds (Hall et al., 2012). Nevertheless, overlap in morphology between diurnal and nocturnal groups means that it is possible to identify individual diurnal and nocturnal bird species that have identical relative cornea sizes. This observation does not refute the fact that, as a group, nocturnal birds have demonstrably larger corneas than diurnal birds as an adaptation for greater light gathering ability at night (Hall et al., 2012). For the same reason, Ruth and colleagues’ (2016) comparisons of individual taxa drawn ad libitum from a larger comparative sample do little to advance the claim that our (Russo and Kirk, 2013) methods failed to demonstrate a relationship between FMP and locomotion and/or trunk posture.

4.2. Objective #1: basioccipital ratio

Despite what we identify as shortcomings in the analysis of Ruth et al. (2016), we regard the question of whether changes in

masticatory anatomy influenced the metrics of FMP used in our original analysis (Russo and Kirk, 2013) as well worth addressing quantitatively with a large comparative sample. It is correct to observe that the three reference points that we used to measure basion position (i.e., anterior margin of the temporal fossa, posterior aspect of the hard palate at midline, and posterior aspect of the last adult molar crown) might be expected to shift in position relative to other cranial structures as a result of selection acting on the masticatory apparatus. We initially attempted to address this issue by demonstrating that, within hominoids, our ratio measures of FMP were positively correlated with measures of basion relative to the bicarotid chord (Table 2 in Russo and Kirk, 2013). In the present study, we quantified basion position using a landmark that is plausibly not primarily influenced by selection on masticatory apparatus: the spheno-occipital synchondrosis. The distance between basion and the spheno-occipital synchondrosis at midline (i.e., sphenobasion) is effectively a measurement of basioccipital length. Although reorganization of the masticatory system could theoretically influence any aspect of cranial morphology, the basioccipital develops as part of the embryonic chondrocranium and is well removed from the more rostral dento-gnathic structures of the splanchnocranium. The basioccipital also has no direct contact with the muscles of mastication, but does provide large insertion sites for the longus capitis and rectus capitis anterior (Gray, 1918). It also provides a small site of origin for the superior pharyngeal constrictor (Gray, 1918). Any evolutionary changes in basioccipital morphology associated with muscular attachment sites are therefore more likely to be the result of selection on muscles that move the head relative to the neck rather than selection on the muscles of mastication.

If bipeds are characterized by a forward shift of the foramen magnum as we initially concluded (Russo and Kirk, 2013), then we expected bipedal species within each clade to exhibit significantly lower basioccipital ratios (i.e., shorter basioccipital lengths relative to cranial size) than their quadrupedal close relatives. Our expectations were confirmed using both the taxa in our original comparative sample (Tables 1 and 2; Fig. 3A, B and D), as well as our new measurements of anomaluroid rodents included to address Objective #3 (Table 1; Fig. 4D; see also Figs. 2 and 5). This signal is strongest for hominoids and rodents, with many modern human individuals and bipedal rodent species exhibiting basioccipital ratios below the ranges of their quadrupedal close relatives. By comparison, although bipedal and quadrupedal diprotodont marsupials differ significantly and in the expected direction, their ranges completely overlap, suggesting that the basioccipital ratio may be of less utility as an indicator of bipedalism in fossil diprotodonts compared to fossil hominoids and rodents. We also found that orthograde strepsirrhines have smaller basioccipital ratios than do non-orthograde strepsirrhines (Fig. 3C). This result provides additional support for the hypothesis that an anteriorly positioned foramen magnum may also be functionally linked to orthograde trunk postures in primates (Kimbel and Rak, 2010; Russo and Kirk, 2013).

These results evaluating basion position relative to the spheno-occipital synchondrosis closely match our findings obtained using three other reference landmarks (i.e., the anterior margin of the temporal fossa, posterior aspect of the hard palate at midline, and posterior aspect of the last adult molar crown; Russo and Kirk, 2013). Because the basioccipital ratio is not expected to be strongly influenced by selection on the masticatory system, the close concordance among all four metrics of relative basion position suggests that our initial observed differences between mammalian bipeds and quadrupeds in molar ratio, temporal fossa ratio, and palate ratio (Russo and Kirk, 2013) probably do not reflect differences in masticatory anatomy (Ruth et al., 2016). Regardless of

how we have quantified relative basion position, our results consistently demonstrate that bipedal/orthograde species have foramina magna that are significantly more anteriorly positioned than quadrupedal/non-orthograde species within each of several major mammalian clades: diprotodont marsupials, heteromyid rodents, dipodid rodents, anomaluroid rodents, strepsirrhine primates, and hominoid primates. Accordingly, these findings reinforce our original conclusion that both bipedal locomotion and orthograde trunk postures are functionally linked to more anteriorly positioned foramina magna in mammals (Russo and Kirk, 2013). Additionally, the results obtained here using basioccipital ratios indicate that such forward shifts may have been achieved in parallel in multiple mammalian groups at least partly through shortening of the basioccipital relative to cranial size (but see Kimbel et al., 2014).

4.3. Objective #2: effect of relative brain size on FMP and FMA

Ruth et al. (2016) dismissed our prior finding that orthograde strepsirrhines have more anteriorly positioned foramina magna than non-orthograde strepsirrhines (Russo and Kirk, 2013) based on their observation that orthograde and non-orthograde strepsirrhines do not differ significantly in FMA. However, Ruth et al. (2016: 48) did find a significant relationship between FMA and the ratio of brain weight to body weight (their “encephalization ratio”, or ER) in strepsirrhines using “a standard linear regression of FMA on ER”. As a result, they concluded that their findings for strepsirrhines support “the hypothesis that relative brain size influences FM position” (Ruth et al., 2016: 49).

Both the rejection of our prior findings for strepsirrhines (Russo and Kirk, 2013) and the conclusion that relative brain size influences foramen magnum position (Ruth et al., 2016) are predicated on the untested assumption that FMA reflects FMP, which we discuss below. However, an additional problem with the ER used by Ruth et al. (2016) as a metric of relative brain size is the fact that this ratio changes systematically with body mass due to interspecific negative allometry in the relationship between brain size and body size across mammals (Martin, 1981; Boddy et al., 2012). In other words, larger species are expected to have lower ERs than smaller species simply due to scaling effects (Jerison, 1973; Martin, 1981). In fact, the largest-bodied strepsirrhine taxon, *Indri indri* (5.83–6.84 kg; Smith and Jungers, 1997), in Ruth et al.’s (2016; their Table 3) sample exhibits the lowest ER value (0.57) while the smallest-bodied strepsirrhine taxon, *Microcebus rufus* (0.042–0.043 kg; Smith and Jungers, 1997), exhibits the highest ER value (4.14). Taxa more similar in body size (e.g., *Propithecus verreauxi* [2.95 kg–3.25 kg] and *Varecia variegata* [3.52–3.65 kg]) possess more similar ER values (0.92 and 0.93, respectively). It is unclear to what extent the findings of Ruth et al. (2016) could have been influenced by independent correlations between body mass and both FMA and brain weight. In this study, we directly examined the relationship between both FMP and FMA and multiple metrics of relative brain size. In order to minimize any influence of brain/body allometry on our findings, we evaluated relative brain size as an encephalization quotient (EQ), in which brain size is expressed in proportion to that expected for a typical mammal of comparable body mass (Boddy et al., 2012). We also expressed encephalization relative to two measures of palate size (Ross and Ravosa, 1993; Bastir et al., 2010) in order to better address the hypothesis of Biegert (1957, 1963) that FMP is influenced by brain size relative to masticatory apparatus size.

Results for the effect of encephalization on FMA and FMP varied by clade. In rodents, we found no significant relationship between FMA and EQ, but we did find a significant relationship between FMA and the cube root of ECV divided by palate length, with the

predictor trait accounting for just over half ($r^2 = 53\%$) of the observed variance in FMA. However, it is worth noting that this relationship was considerably weakened with the inclusion of palate width ($r^2 = 28\%$), and the relationship is not significant with the removal of *Chaetodipus hispidus*, which exhibits a substantially lower measure of FMA (Ruth et al., 2016) than any other rodent in the sample. We also found a single significant relationship for FMP: that between basioccipital ratio and the cube root of ECV divided by palate length. However, the fact that basioccipital ratio is not significantly related to either EQ alone or to the cube root of ECV divided by the geometric mean of palate length and width suggests that relative brain size probably has little appreciable influence on FMP in rodents. In marsupials, we found no significant relationship between any metric of FMP or FMA and any measure of relative brain size.

By comparison, strepsirrhines reveal a more complex relationship between FMP, FMA, and encephalization than do either rodents or marsupials. FMA in strepsirrhines is not significantly related to EQ alone, but FMA is negatively correlated with both metrics of ECV relative to palate size. These findings suggest that although encephalization in isolation does not influence strepsirrhine FMA, strepsirrhine species with large palates for their relative brain sizes tend to have more posteriorly-facing foramina magna. This result lends some support for Biegert’s hypotheses about the interrelatedness of face size, neocortex size, and the configuration of the FM, wherein a large masticatory apparatus is proposed to inhibit anterior FM migration and inclination (Biegert, 1957, 1963; see also Russo and Kirk, 2013 for discussion). By comparison, none of the relationships between EQ and our four metrics of FMP was significant in strepsirrhines. We did, however, observe that molar ratio is significantly related to the cube root of ECV divided by palate length, and the cube root of ECV divided by the geometric mean of palate length and width. In both cases the direction of the relationship fits the expectations of Biegert (1957, 1963), but the explanatory power of the two metrics is small ($r^2 = 0.32$ and 0.22 , respectively). We also found that strepsirrhine basioccipital ratio is significantly related to ECV relative to palate length. However, the strength of this relationship is small ($r^2 = 0.35$) and it becomes non-significant when palate width is also considered.

Taken as a whole, our results do not lend support to the contention of Ruth et al. (2016) that our prior findings for strepsirrhines (Russo and Kirk, 2013) are the result of interspecific differences in relative brain size. Our four metrics of relative FMP (molar ratio, palate ratio, temporal fossa ratio, and basioccipital ratio) have no statistically significant relationship with EQ in strepsirrhines, rodents, or marsupials. Notably, our finding of a non-significant relationship between FMA and EQ in all clades is at odds with the report of a significant relationship between FMA and ER in strepsirrhines (Ruth et al., 2016). The discordance of these results may be attributable to the use of differing measures of relative brain size and/or our use of phylogenetically informed methods. Furthermore, of the 24 comparisons between FMP and brain size relative to palate size in our comparative sample, only four were statistically significant (Tables 3–5). These results suggest that EQ alone has no discernible effect on FMP or FMA. Similarly, brain size relative to palate size may have a weak influence on FMP, but any such effects are not evident in all metrics of FMP (e.g., palate ratio and temporal fossa ratio) and are inconsistent between clades.

4.4. Objective #3: anomaluroid rodents

In order to broaden the scope of our previous comparative analysis (Russo and Kirk, 2013), we extended our analyses of FMP to an additional clade – the Anomaluroida. Encompassing both

anomalures (*Anomalurus* spp.) and springhares (*Pedetes* spp.), anomaluroids represent a third clade of rodents in which bipedalism evolved independently of that in dipodids and heteromyids, and thus provide an additional opportunity to test the hypothesized functional association between a forward shift in FMP and bipedalism. Our results for anomaluroids largely support our prior findings for dipodid and heteromyid rodents (Russo and Kirk, 2013), with bipedal *Pedetes* exhibiting significantly lower molar ratios, palate ratios, and basioccipital ratios than quadrupedal/gliding *Anomalurus*. These results demonstrate that basion is more anteriorly positioned relative to the posterior molar, posterior hard palate, and spheno-occipital synchondrosis in bipedal anomaluroids than in quadrupedal anomaluroids. This finding is particularly interesting in light of the fact that, as with bipedal marsupials and other bipedal rodents (see Russo and Kirk, 2013, their Figure 7, and citations therein), the trunk of *Pedetes* may be held sub-horizontally during rest or locomotion (e.g., Fig. 2D). As previously noted (Strait and Ross, 1999; Russo and Kirk, 2013), there are limitations to using gross postural categories (e.g., orthograde versus pronograde) because the trunk does not directly articulate with the basicranium. As such, a comprehensive understanding of how FM position is functionally related to variation in head/neck posture during foraging and traveling, and to resisting the forces engendered by saltation in rodents and macropodids (Du Brul, 1950), will require additional data on cervical vertebral morphology, kinetics, and kinematics in mammalian bipeds.

Contrary to our expectations, we found that *Anomalurus* has a significantly lower temporal fossa ratio than *Pedetes*. This result may be attributable to differences between *Anomalurus* and *Pedetes* in temporal fossa morphology. Like most rodents (E.C.K. pers. obs.), the anterior margin of the temporal fossa in *Anomalurus* is either transversely aligned with or immediately anterior to the mesial-most cheek teeth (Fig. 5). By contrast, the anterior margin of the temporal fossa in *Pedetes* is displaced far anterior to the mesial-most cheek teeth (Fig. 5). This morphology is less common in rodents (E.C.K. pers. obs.) and is presumably a derived condition. Due to these differences in temporal fossa morphology, the distance between basion and the anterior temporal fossa is relatively greater in *Pedetes* than in *Anomalurus*. This result provides one example supporting the contention of Ruth et al. (2016) that our ratios quantifying FMP may be influenced by changes in the relative position of the reference point instead of basion. However, rather than concluding that none of our ratios effectively quantifies FMP, it is our view that this example underscores the importance of evaluating FMP relative to multiple fixed reference points in the context of a broad comparative sample. In total, the comparative data on FMP for rodents presented here (Figs. 3A and 4) lend strong support to our initial conclusion that bipedal species tend to exhibit more anteriorly positioned foramina magna than quadrupedal species (Russo and Kirk, 2013).

In this context, it is also worth noting that our findings for anomaluroids cannot be attributed to hypertrophy of the auditory bullae, as Ruth et al. (2016) argued with respect to our prior results for heteromyid and dipodid rodents (Russo and Kirk, 2013). Bulla size is relatively much larger in quadrupedal/gliding *Anomalurus* than in bipedal *Pedetes* (see Fig. 5), but as noted above *Pedetes* has a more anteriorly positioned foramen magnum than *Anomalurus* (Fig. 4). This pattern for anomaluroids is the opposite of that observed for dipodids and heteromyids, in which bipedal species with bullar hypertrophy (see Ruth et al., 2016) also tend to have relatively anteriorly positioned foramina magna (Russo and Kirk, 2013). These findings are also consistent with our analyses of basioccipital ratio (Figs. 3A and 4D), which demonstrate that bipedal species in all three of the rodent clades that we examined tend to have relatively shorter basioccipital lengths and more anteriorly positioned foramina magna than quadrupedal rodents. As

a result, the available comparative data suggest that there is no systematic influence of auditory bulla size on FMP in rodents.

4.5. Objective #4: relationship between FMP and FMA

As noted above, criticism of our prior analysis (Russo and Kirk, 2013) by Ruth et al. (2016) is predicated partly on the notion that these authors have more accurately measured FMP by (paradoxically) measuring FMA instead. For example, on the basis of a “side-by-side comparison of the species with the highest and lowest FMAs”, Ruth and colleagues “conclude that FMA is a more appropriate measure of FM position” than molar ratio, temporal fossa ratio, or palate ratio (Ruth et al., 2016: 46–47). In the absence of an explicit and more systematic analysis of the relationship between FMA and FMP, we regard this approach as logically unsound and the conclusion as premature. FMP must be measured relative to other cranial landmarks in order to determine if the foramen magnum is (or is not) anteriorly shifted in bipeds (i.e., the primary hypothesis that we tested; Russo and Kirk, 2013). In other words, it seems self-evident to us that the best way to test if FMP is associated with bipedal locomotion and/or orthograde postures is to measure FMP directly rather than by measuring a third variable that may or may not be correlated with FMP. In the present study, we have directly evaluated the claim that FMA reliably predicts FMP. To do so, we first examined metrics of FMP and FMA deemed standard in the paleoanthropological literature (e.g., basion position relative to the bicarotid chord) within a large sample ($n = 198$ individuals) of hominoids. We found no relationship between FMA and either the bicarotid index or Weidenreich index among non-human hominoids. Among all hominoids, we observed a significant relationship between the Weidenreich index and FMA, but not between the bicarotid index and FMA. These results indicate that any analysis of the relationship between FMA and FMP in hominoids will be strongly influenced by both the metrics used and the inclusion of modern humans within the sample. In the case of our single significant result, it is worth mentioning that the Weidenreich index measures the position of the posterior margin of the foramen magnum relative to the posterior margin of the braincase (Weidenreich, 1943). By contrast, the bicarotid index measures the anterior margin of the foramen magnum relative to a more anteriorly located reference line (i.e., the bicarotid chord). Given the differences between modern humans and other extant hominoids in the degree of posterior projection of the braincase relative to the position of the foramen magnum, it is not surprising that our analyses of hominoids yielded different results for the Weidenreich index and bicarotid index. Changes in human FMA may be generated by an inferior shift of opisthion in relation to the Frankfort Horizontal as a result of expansion of the neurocranium in humans (Kimbel et al., 2004). In short, our findings show that FMA is significantly related to FMP in living hominoids when foramen magnum position is measured relative to the posteriormost extent of the cranial vault, but this relationship is not significant when foramen magnum position is measured relative to the bicarotid chord. These results probably reflect the fact that modern humans have both (1) more anteroinferiorly facing foramina magna and (2) more posteriorly projecting braincases than other extant hominoids. These differences between methods of quantifying FMP also further underscore the importance of explicitly specifying a fixed frame of reference by which the relative position of the foramen magnum should be measured.

Our results for the relationship between FMA and ratio measures of FMP in the broader mammalian sample also varied by clade. We found no relationship between FMA and any of our four metrics of FMP among marsupials. In rodents, only the basioccipital ratio was significantly, though weakly ($r^2 = 0.31$), influenced by

FMA. Among strepsirrhines, the relationship was more complicated, with two (palate ratio and basioccipital ratio) of our four metrics of FMP showing significant relationships with FMA. However, in both cases FMA accounted for less than half ($r^2 = 0.33$ [palate] and 0.41 [basioccipital]) of the observed variance in FMP. Having demonstrated a lack of a relationship between FMP and FMA among non-human hominoids for both the bicarotid and Weidenreich indices, and among all hominoids for the bicarotid index, as well as a lack of a relationship between FMP and FMA in three quarters of the analyses in the comparative mammalian sample, we find the assertion by Ruth et al. (2016) that FMA accurately captures FMP to be untenable.

5. Conclusions

In our previous study (Russo and Kirk, 2013), we used three metrics of relative basion position to demonstrate that an anteriorly positioned foramen magnum is a basicranial feature shared by multiple clades of bipedal mammals. In this study, results from quantitative analyses of an additional metric of relative basion position (the basioccipital ratio) in our former comparative sample (Russo and Kirk, 2013), and of all four metrics of FMP in an additional rodent clade (Anomaluroidea), corroborate our earlier findings that bipedal rodents, marsupials, and hominoid primates have more anteriorly positioned foramina magna than their quadrupedal close relatives. Orthograde strepsirrhines also have more anteriorly positioned foramina magna than non-orthograde strepsirrhines. Findings of the present study further reveal that relative brain size alone (EQ) has no discernible effect on FMP or FMA. Brain size relative to palate size may have a weak influence on FMP in some clades, but any such effects are not evident in all metrics of FMP and are inconsistent between clades. Furthermore, tests of the relationship between FMA and FMP in extant hominoids measured using metrics standard in the paleoanthropological literature show inconsistent results that are dependent on metric choice and the inclusion of modern humans in the comparative sample. Similarly, the relationships between FMA and our four metrics of FMP are nonexistent or weak across rodents, marsupials, and strepsirrhine primates. In our view, these findings largely invalidate the critiques of our prior analysis (Russo and Kirk, 2013) made by Ruth et al. (2016) because these authors did not measure FMP directly and instead relied on FMA as an untested proxy for FMP. At the same time, the results of our analyses lend support to the possibility that the causes of the anterior position and antero-inferior inclination of the modern human foramen magnum may result from different selective pressures. Reports that some *Australopithecus* specimens appear to exhibit human-like foramen magnum positions but more chimpanzee-like foramen magnum orientations (Kimbel and Rak, 2010) could indicate that the evolution of FMP and FMA in hominins is not closely coupled. Indeed, given the many possible selective influences on basicranial morphology in hominoids and other mammals, it is perhaps not surprising that our data provide little support for the hypothesis that changes in FMP are correlated with changes in FMA.

Acknowledgements

We would like to thank the Editor, Assistant Editor, and three anonymous reviewers for the constructive comments that considerably improved the manuscript. We would also like to acknowledge the several sources from which we were able to include images of anomaluroid rodents, including Nik Borrow, C. Smith and the American Society of Mammalogists Mammal Images Library, and Bernard Dupont (Wikimedia Commons). We are grateful to Christina Chan, Tara Galusha, Jordan Guerra, and Iain Mawhinney

for assistance with data collection and literature research, and Jeroen B. Smaers and W. Andrew Barr for statistical advice. Finally, thanks are also owed to Ruth et al. (2016) for encouraging us to think more critically about basicranial morphology. Part of this research was funded by a Leakey Foundation General Research Grant.

Supplementary Online Material

Supplementary online material related to this article can be found at <http://dx.doi.org/10.1016/j.jhevol.2017.01.018>.

References

- Ahern, J.C., 2005. Foramen magnum position variation in *Pan troglodytes*, Pliocene hominids, and recent *Homo sapiens*: implications for recognizing the earliest hominids. *Am. J. Phys. Anthropol.* 127, 267–276.
- Arnold, C., Matthew, L.J., Nunn, C.L., 2010. The 10kTrees website: A new online resource for primate phylogeny. *Evol. Anthropol.* 19, 114–118.
- Ashwell, K., 2008. Encephalization of Australian and New Guinean marsupials. *Brain Behav. Evol.* 71, 181–199.
- Bastir, M., Rosas, A., Stringer, C., Cuétara, J.M., Kruszynski, R., Weber, G.W., Ross, C.F., Ravosa, M.J., 2010. Effects of brain and facial size on basicranial form in human and primate evolution. *J. Hum. Evol.* 58, 424–431.
- Biegert, J., 1957. Der Formwandel des Primatenschädels und seine Beziehungen zur ontogenetischen Entwicklung und den phylogenetischen Spezialisierungen der Kopforgane. *Gegenbr. Morph. Jahrb.* 98, 77–199.
- Biegert, J., 1963. The evaluation of characteristics of the skull, hands and feet for primate taxonomy. In: Washburn, S.L. (Ed.), *Classification and Human Evolution*. Aldine, Chicago, pp. 116–145.
- Bininda-Emonds, O.R., Cardillo, M., Jones, K.E., MacPhee, R.D., Beck, R.M., Grenyer, R., Price, S.A., Vos, R.A., Gittleman, J.L., Purvis, A., 2007. The delayed rise of present-day mammals. *Nature* 446, 507–512.
- Boddy, A., McGowen, M., Sherwood, C., Grossman, L., Goodman, M., Wildman, D., 2012. Comparative analysis of encephalization in mammals reveals relaxed constraints on anthropoid primate and cetacean brain scaling. *J. Evol. Bio.* 25, 981–994.
- Broca, P., 1872. Sur la direction du trou occipital; description du niveau occipital et du goniomètre occipital. *Bull. Soc. Anthropol. Paris* 7, 649–668.
- Brunet, M., 2002. Reply to: Palaeoanthropology (communication arising): *Sahelanthropus* or "*Sahelpithecus*"? *Nature* 419, 582.
- Brunet, M., Guy, F., Pilbeam, D., Mackaye, H.T., Likius, A., Ahounta, D., Beauvilain, A., Blondel, C., Bocherens, H., Boisserie, J.R., de Bonis, L., Coppens, Y., Dejax, J., Denys, C., Düringer, P., Eisenmann, V., Gongdibé, F., Fronty, P., Geraads, D., Lehmann, T., Lihoreau, F., Louchart, A., Mahamat, A., Merceron, G., Mouchelin, G., Otero, O., Pelaez Campomanes, P., Ponce de León, M., Rage, J.-C., Sapanet, M., Schuster, M., Sudre, J., Tassy, P., Valentin, X., Vignaud, P., Viriot, L., Zazzo, A., Zollikofer, C., 2002. A new hominid from the Upper Miocene of Chad, Central Africa. *Nature* 418, 145–151.
- Butynski, T.M., 1984. Nocturnal ecology of the springhare, *Pedetes capensis*, in Botswana. *Afr. J. Ecol.* 22, 7–22.
- Butynski, T.M., 2013. *Pedetes capensis* Southern African springhare. In: Happold, D. (Ed.), *Mammals of Africa*. Bloomsbury Publishing, London, pp. 619–624.
- Butynski, T.M., Mattingly, R., 1979. Burrow structure and fossorial ecology of the springhare *Pedetes capensis* in Botswana. *Afr. J. Ecol.* 17, 205–215.
- Coddington, J.A., 1994. *The Roles of Homology and Convergence in Studies of Adaptation, Phylogenetics and Ecology*. Academic Press, London, pp. 53–78.
- Dart, R., 1925. *Australopithecus africanus*: the man-ape of southern Africa. *Nature* 2884, 195–199.
- Daubenton, L.J.M., 1764. Mémoire sur les différences de la situation du grand trou occipital dans l'homme et dans les animaux. *Mem. Acad. Sci.* 66, 568–575.
- Du Bruil, E.L., 1950. Posture, locomotion and the skull in Lagomorpha. *Am. J. Anat.* 87, 277–313.
- Fabre, P.-H., Hautier, L., Dimitrov, D., Douzery, E.J., 2012. A glimpse on the pattern of rodent diversification: a phylogenetic approach. *BMC Evol. Biol.* 12, 1–19.
- Fabre, P.-H., Jönsson, K.A., Douzery, E.J., 2013. Jumping and gliding rodents: mitochondrial affinities of Pedetidae and Anomaluridae deduced from an RNA-Seq approach. *Gene* 531, 388–397.
- Gray, H., 1918. *Anatomy of the Human Body*. Lea & Febiger, Philadelphia and New York.
- Guy, F., Lieberman, D.E., Pilbeam, D., de León, M.P., Likius, A., Mackaye, H.T., Vignaud, P., Zollikofer, C., Brunet, M., 2005. Morphological affinities of the *Sahelanthropus tchadensis* (Late Miocene hominid from Chad) cranium. *Proc Natl Acad Sci U S A* 102, 18836–18841.
- Hafner, M.S., Hafner, J.C., 1984. Brain size, adaptation and heterochrony in geomyoid rodents. *Evolution* 38, 1088–1098.
- Hall, M.L., Kamilar, J.M., Kirk, E.C., 2012. Eye shape and the nocturnal bottleneck of mammals. *P. Roy. Soc. Lond. B Bio.* 279, 4962–4968.

- Harvey, P.H., Pagel, M.D., 1991. *The Comparative Method in Evolutionary Biology*. Oxford University Press, Oxford.
- Heritage, S., Fernández, D., Sallam, H.M., Cronin, D.T., Echube, J.M.E., Seiffert, E.R., 2016. Ancient phylogenetic divergence of the enigmatic African rodent *Zenkerella* and the origin of anomalurid gliding. *PeerJ* 4, e2320.
- IBM Corp., 2013. Released 2013. IBM SPSS Statistics for Windows, Version 22.0. IBM Corp, Armonk, NY.
- Isler, K., Kirk, E.C., Miller, J.M., Albrecht, G.A., Gelvin, B.R., Martin, R.D., 2008. Endocranial volumes of primate species: scaling analyses using a comprehensive and reliable data set. *J. Hum. Evol.* 55, 967–978.
- Jerison, H., 1973. *Evolution of the Brain and Intelligence*. Academic Press, New York.
- Kimbel, W.H., Rak, Y., 2010. The cranial base of *Australopithecus afarensis*: New insights from the female skull. *Phil. Trans. R. Soc.* 365, 3365–3376.
- Kimbel, W.H., Rak, Y., Johanson, D.C., 2004. *The Skull of Australopithecus afarensis*. Oxford University Press, Oxford.
- Kimbel, W.H., Suwa, G., Asfaw, B., Rak, Y., White, T.D., 2014. *Ardipithecus ramidus* and the evolution of the human cranial base. *Proc. Natl. Acad. Sci.* 111, 948–953.
- Luboga, S., Wood, B., 1990. Position and orientation of the foramen magnum in higher primates. *Am. J. Phys. Anthropol.* 81, 67–76.
- Martin, R.D., 1981. Relative brain size and basal metabolic rate in terrestrial vertebrates. *Nature* 293, 57–60.
- Martins, E.P., Hansen, T.F., 1997. Phylogenies and the comparative method: a general approach to incorporating phylogenetic information into the analysis of interspecific data. *Am. Nat.* 149, 646–667.
- Muchlinski, M.N., 2010. A comparative analysis of vibrissa count and infraorbital foramen area in primates and other mammals. *J. Hum. Evol.* 58, 447–473.
- Nowak, R.M., 1999. *Walker's Mammals of the World*, Sixth ed. The Johns Hopkins University Press, Baltimore, Maryland.
- Paradis, E., Claude, J., Strimmer, K., 2004. APE: analyses of phylogenetics and evolution in R language. *Bioinformatics* 20, 289–290.
- Pinheiro, J., Bates, D., DebRoy, S., Sarkar, D., R Core Team, 2014. nlme: Linear and Nonlinear Mixed Effects Models. R package version 3.1-117. Available: <http://CRAN.R-project.org/package=nlme>.
- R Core Team, 2014. R: A language and environment for statistical computing. R Foundation for Statistical Computing, Vienna, Austria. <http://www.R-project.org/>.
- Ross, C.F., Ravosa, M.J., 1993. Basicranial flexion, relative brain size, and facial kyphosis in nonhuman primates. *Am. J. Phys. Anthropol.* 91, 305–324.
- Russo, G.A., Kirk, E.C., 2013. Foramen magnum position in bipedal mammals. *J. Hum. Evol.* 65, 656–670.
- Russo, G.A., Kirk, E., Smaers, J.B., 2016. Elucidating the evolutionary pathways of hominoid and hominin basicranial morphology using a formal phylogenetic comparative primate approach. *Am. J. Phys. Anthropol.* 159, 276.
- Ruth, A.A., Raghanti, M.A., Meindl, R.S., Lovejoy, C.O., 2016. Locomotor pattern fails to predict foramen magnum angle in rodents, strepsirrhine primates, and marsupials. *J. Hum. Evol.* 94, 45–52.
- Samuels, J.X., Van Valkenburgh, B., 2008. Skeletal indicators of locomotor adaptations in living and extinct rodents. *J. Morphol.* 269, 1387–1411.
- Schaefer, M.S., 1999. Brief communication: Foramen magnum–carotid foramina relationship: Is it useful for species designation? *Am. J. Phys. Anthropol.* 110, 467–471.
- Schultz, A.H., 1942. Conditions for balancing the head in primates. *Am. J. Phys. Anthropol.* 29, 483–497.
- Schultz, A.H., 1955. The position of the occipital condyles and of the face relative to the skull base in primates. *Am. J. Phys. Anthropol.* 13, 97–120.
- Silva, M., Downing, J.A., 1995. *CRC Handbook of Mammalian Body Masses*. CRC Press, Boca Raton, Florida.
- Smith, R.J., Jungers, W.L., 1997. Body mass in comparative primatology. *J. Hum. Evol.* 32, 523–559.
- Strait, D.S., Ross, C.F., 1999. Kinematic data on primate head and neck posture: implications for the evolution of basicranial flexion and an evaluation of registration planes used in paleoanthropology. *Am. J. Phys. Anthropol.* 108, 205–222.
- Suwa, G., Asfaw, B., Kono, R.T., Kubo, D., Lovejoy, C.O., White, T.D., 2009. The *Ardipithecus ramidus* skull and its implications for hominid origins. *Science* 326, 68.
- Topinard, P., 1890. *Anthropology*. Chapman and Hall, London.
- Weidenreich, F., 1943. The skull of *Sinanthropus pekinensis*: A comparative study on a primitive hominid skull. *Palaeontologia Sinica New Series D no. 10, Whole Series no. 127*.
- White, T.D., Suwa, G., Asfaw, B., 1994. *Australopithecus ramidus*, a new species of early hominid from Aramis, Ethiopia. *Nature* 371, 306–312.
- Wilson, D.E., Reeder, D.M., 2005. *Mammal Species of the World: a Taxonomic and Geographic Reference*. The Johns Hopkins University Press, Baltimore, Maryland.
- Wolpoff, M.H., Senut, B., Pickford, M., Hawks, J., 2002. Palaeoanthropology (communication arising): *Sahelanthropus* or “*Sahelpithecus*”? *Nature* 419, 581–582.
- Wolpoff, M.H., Hawks, J., Senut, B., Pickford, M., Ahern, J., 2006. An ape or the ape: is the Toumaï cranium TM 266 a hominid. *PaleoAnthropology* 2006, 36–50.